Divergence of the floral a-function between an asterid and a rosid species

Patrice Morel, Klaas Heijmans, Frédérique Rozier, Jan Zethof, Sophy Chamot, Suzanne Rodrigues Bento, Aurélie Vialette-Guiraud, Pierre Chambrier, Christophe Trehin, Michiel Vandenbussche

The Plant Cell, Vol. 29: 1605–1621, July 2017, www.plantcell.org © 2017 ASPB.

Divergence of the Floral A-Function between an Asterid and a Rosid Species[OPEN]

Patrice Morel,[a] Klaas Heijmans,[b] Frédérique Rozier,[a] Jan Zethof,[b] Sophy Chamot,[a] Suzanne Rodrigues Bento,[a] Aurélie Vialette-Guiraud,[a] Pierre Chambrier,[a] Christophe Trehin,[a] and Michiel Vandenbussche[a,1]

[a] Laboratoire Reproduction et Développement des Plantes, Univ Lyon, ENS de Lyon, UCB Lyon 1, CNRS, INRA, F-69342 Lyon, France

[b] Institute for Water and Wetland Research, Radboud University Nijmegen, 6525AJ Nijmegen, The Netherlands

ORCID IDs: 0000-0003-1690-8032 (P.M.); 0000-0003-1888-3094 (S.R.B.); 0000-0002-6430-7429 (A.V.-G.); 0000-0001-5390-1345 (P.C.); 0000-0003-4045-6160 (C.T.); 0000-0002-4192-7369 (M.V.)

The ABC model is widely used as a genetic framework for understanding floral development and evolution. In this model, the A-function is required for the development of sepals and petals and to antagonize the C-function in the outer floral whorls. In the rosid species *Arabidopsis thaliana*, the AP2-type AP2 transcription factor represents a major A-function protein, but how the A-function is encoded in other species is not well understood. Here, we show that in the asterid species petunia (*Petunia hybrida*), *AP2B/BLIND ENHANCER* (*BEN*) confines the C-function to the inner petunia floral whorls, in parallel with the microRNA *BLIND*. *BEN* belongs to the TOE-type *AP2* gene family, members of which control flowering time in Arabidopsis. In turn, we demonstrate that the petunia AP2-type *REPRESSOR OF B-FUNCTION* (*ROB*) genes repress the B-function (but not the C-function) in the first floral whorl, together with *BEN*. We propose a combinatorial model for patterning the B- and C-functions, leading to the homeotic conversion of sepals into petals, carpels, or stamens, depending on the genetic context. Combined with earlier results, our findings suggest that the molecular mechanisms controlling the spatial restriction of the floral organ identity genes are more diverse than the well-conserved B and C floral organ identity functions.

INTRODUCTION

More than two decades ago, the classic ABC model (Bowman et al., 1991; Coen and Meyerowitz, 1991) was formulated to describe how the identity of each of the floral organs (sepals, petals, stamens, and carpels) is acquired by different combinations of three classes of homeotic gene functions, called A, B, and C. This model, based on floral homeotic mutants in *Arabidopsis thaliana* and snapdragon (*Antirrhinum majus*), proposes that the expression of A alone specifies sepals, A and B together petals, B and C stamens, and C alone carpels. The ABC model has been widely used as a framework for understanding floral development and evolution. The B- and C-function genes, initially identified in both Arabidopsis and snapdragon (Sommer et al., 1990; Yanofsky et al., 1990; Jack et al., 1992; Tröbner et al., 1992; Bradley et al., 1993; Goto and Meyerowitz, 1994; Causier et al., 2005), have been well characterized at the molecular level in a diverse range of species (Krizek and Fletcher, 2005), including petunia (*Petunia hybrida*) (Angenent et al., 1993; van der Krol et al., 1993; Kater et al., 1998; Kapoor et al., 2002; Vandenbussche et al., 2004; Rijpkema et al., 2006; Heijmans et al., 2012). In contrast, how the A-function is encoded in species other than Arabidopsis remains poorly understood. Moreover, the exact definition of the A-function itself has been a subject of debate in more recent years (Litt, 2007; Causier et al., 2010). The classical A-function is proposed to play a dual role: to be required for normal sepal and petal development and to antagonize the expression of the C-function in whorls 1 and 2. Accurate patterning of the floral organ identity genes is indeed crucial for floral development since their misexpression leads to homeotic conversion of one floral organ type into another. In Arabidopsis, the AP2 (APETALA2) transcription factor represents one of the major A-function genes: Loss of *AP2* function results in the transformation of the sepals into carpelloid structures or leaf-like organs (allele dependent), and petals are either absent or transformed into stamen-like structures due to ectopic C-class activity in the perianth (Kunst et al., 1989; Bowman et al., 1991; Drews et al., 1991; Jofuku et al., 1994). More recently, it has been shown that AP2 is regulated by the microRNA *miR172* (Chen, 2004), and the roles of *AP2* and *miR172* have been further refined and extended (Wollmann et al., 2010; Dinh et al., 2012; Krogan et al., 2012). So far, efforts to associate a similar dual A-function to the *AP2*-like genes *LIPLESS1* (*LIP1*)/*LIP2* from snapdragon (Keck et al., 2003) and *AP2A* (Maes et al., 2001) from petunia were unsuccessful: No C-patterning defects were observed in petunia *ap2a* or snapdragon *lip1 lip2* mutants. However, like *AP2*, *LIP* genes were shown to play a role in sepal, petal, and ovule development, while *ap2a* mutants displayed a wild-type phenotype. Nevertheless, other mutants with a partial A-function mutant phenotype were found in petunia and snapdragon, called *blind* (*bl*) (Vallade et al., 1987) and *fistulata* (*fis*) (McSteen et al., 1998), respectively. In both mutants, the 2nd whorl petals are converted to antheroid structures due to expansion of the C-function domain in the outer whorls. We showed that *BL* and *FIS* encode homologous miRNAs from the

[1] Address correspondence to michiel.vandenbussche@ens-lyon.fr.
The author responsible for distribution of materials integral to the findings presented in this article in accordance with the policy described in the Instructions for Authors (www.plantcell.org) is: Michiel Vandenbussche (michiel.vandenbussche@ens-lyon.fr).
[OPEN] Articles can be viewed without a subscription.
www.plantcell.org/cgi/doi/10.1105/tpc.17.00098

miR169 family, regulating a subset of NF-YA transcription factors, the derepression of which is proposed to lead to an expansion of the C-expression domain into the outer floral whorls (Cartolano et al., 2007). This revealed an unrelated C-function patterning mechanism in petunia and snapdragon compared with Arabidopsis *AP2* function. Together, this suggests that the genetic basis of the A-function may have undergone major evolutionary changes between Arabidopsis (a Rosid species) and petunia and snapdragon (Asterid species). Rosids and Asterids represent the two largest higher eudicot clades that separated >100 million years ago (Moore et al., 2010).

Interestingly, even though the C-function genes are ectopically expressed in the first whorl of *bl* and *fis* mutants (Tsuchimoto et al., 1993; Kater et al., 1998; Rijpkema et al., 2006; Cartolano et al., 2007), this does not lead to a homeotic conversion of sepals into carpels, in contrast to what would be predicted by the ABC model. This indicates that one or more additional factors exist that prevent carpel development in the first whorl, acting either alone or redundantly with *BL/FIS.* Here, we report the characterization and cloning of such a factor in petunia, *AP2B* (renamed *BLIND ENHANCER* [*BEN*]), which we identified as a spontaneous recessive mutation in the *bl* background. Interestingly, *ben bl* mutants display a full homeotic conversion of sepals into carpels similar to strong Arabidopsis *ap2* alleles, demonstrating that *AP2B/BEN* represses the C-function together with *BL*. We show that *BEN* is a member of the *euAP2* lineage, a subgroup of the large AP2/ERF transcription factor family that is characterized by the presence of two AP2 domains and a miR172 target site (Kim et al., 2006). The *euAP2* lineage can be further divided into two different classes called the TOE and AP2 types (Wang et al., 2016). The Arabidopsis A-class gene *AP2* belongs to the AP2 type, together with *TOE3.* Although *BEN* appears to encode the functional equivalent of Arabidopsis *AP2*, *BEN* belongs to the TOE type of the *euAP2* lineage, which in Arabidopsis are represented by *TARGET OF EAT1* (*TOE1*), *TOE2*, *SCHLAFMÜTZE* (*SMZ*), and *SCHNARCHZAPFEN* (*SNZ*). Together with *TOE3*, these genes redundantly act as floral repressors (Aukerman and Sakai, 2003; Jung et al., 2007; Mathieu et al., 2009; Yant et al., 2010), but in contrast to *ben*, loss-of-function mutants for these genes do not display defects in floral organ development. Interestingly, in the absence of the *bl* mutation, single *ben* mutants show a defect in patterning of the B-class genes, a phenotype that in normal forward genetic screens would never have identified *BEN* as a C-patterning factor. Furthermore, by mining the petunia genome sequences (Bombarely et al., 2016), we found that in addition to the previously described *AP2A* gene (Maes et al., 2001), petunia contains two more members of the AP2-type class. It could therefore not be excluded that the absence of an Arabidopsis *ap2*-like phenotype in the previously described single *ap2a* mutants (Maes et al., 2001) is simply due to redundancy and, thus, that petunia *AP2*-type genes potentially might function in a similar manner as Arabidopsis *AP2*. However, in contrast to *BEN*, we did not find any evidence that these three genes are involved in C-function repression in the perianth, although we show that they do play a role in sepal, petal, and ovary development. Surprisingly, we found instead that they function as major B-function repressors in the first floral whorl, redundantly with *BEN*. Combined with earlier results, our findings provide further support for the idea that the molecular mechanisms controlling the spatial restriction of the floral organ identity genes are more diverse compared with the well-conserved B and C floral organ identity functions. Our results extend the genetic framework for studying floral diversity and evolution and offer deeper insight in the evolutionary history of the *AP2* family.

RESULTS

ap2b/ben Completes the Partial A-Function Phenotype of *blind* Mutants

In flowers of the *bl* mutant (Figure 1), petals are homeotically converted into antheroid structures due to the combined expression of the B- and C-function genes in the 2nd whorl. Although the two C-function MADs box genes *pMADS3* and *Floral Binding Protein gene 6* (*FBP6*) are also ectopically expressed in the first whorl of *bl* mutant flowers (Tsuchimoto et al., 1993; Kater et al., 1998; Rijpkema et al., 2006; Cartolano et al., 2007) (Figure 1U), these organs largely retain sepal identity (Figures 1I and 1J), while normally carpels would be expected based on the ABC model. This suggested that one or more additional factors exist that represses the C-function together with *BL*. To isolate such redundant regulators, we introgressed the *bl-1* allele in the W138 *dTph1* transposon high copy number line (Gerats et al., 1990) to perform a secondary mutagenesis screen. We identified a single recessive mutation, named *ben*, which in combination with *bl* leads to the homeotic conversion of all sepals into carpels. These first whorl carpels are fully fused enclosing the inner organs, terminate with a stigma, and internally develop ovaries, bearing wild-type-looking ovules (Figures 1C, 1G, 1K, and 1S). At the cellular level, *ben bl* first whorl organs display the typical stigma and carpel wall epidermal cell types found in wild-type pistils (Figures 1M to 1P).

In all flowers examined, we found that development of the 2nd floral whorl was largely suppressed (Figure 1K), while one or more stamens were strongly underdeveloped or completely missing in the 3rd floral whorl. Together, the phenotype of *ben bl* flowers closely resembles the strongest *ap2* alleles in Arabidopsis (Bowman et al., 1991). Consistent with the observed phenotype, we found an ~4-fold further increase in C-class gene expression levels in *ben bl* first whorl carpels compared with *bl* sepals (Figure 1U). This demonstrates that *BL* and *BEN* together are involved in the repression of C-class gene expression in the first floral whorl and that only in *ben bl* double mutants sufficiently high C-expression levels are reached to provoke homeotic conversion of sepals into carpels. To assess the phenotype of *ben* independently from *bl*, we outcrossed *ben bl* individuals to obtain families in which both *ben* and *bl* separately segregated. Remarkably, *ben* single mutants did not reveal any phenotypic indication that patterning of the C-function was affected, as would normally be expected based on the strong enhancement of the *bl* phenotype by *ben*. In line with that, no upregulation of the C-class genes was detected in the sepals of *ben* single mutants, demonstrating that *BL* fully masks the C-patterning function of *BEN*.

Surprisingly, all *ben* single mutant individuals instead displayed a clear although subtle phenotypic defect, suggesting that *BEN* in a wild-type background is involved in the patterning of the

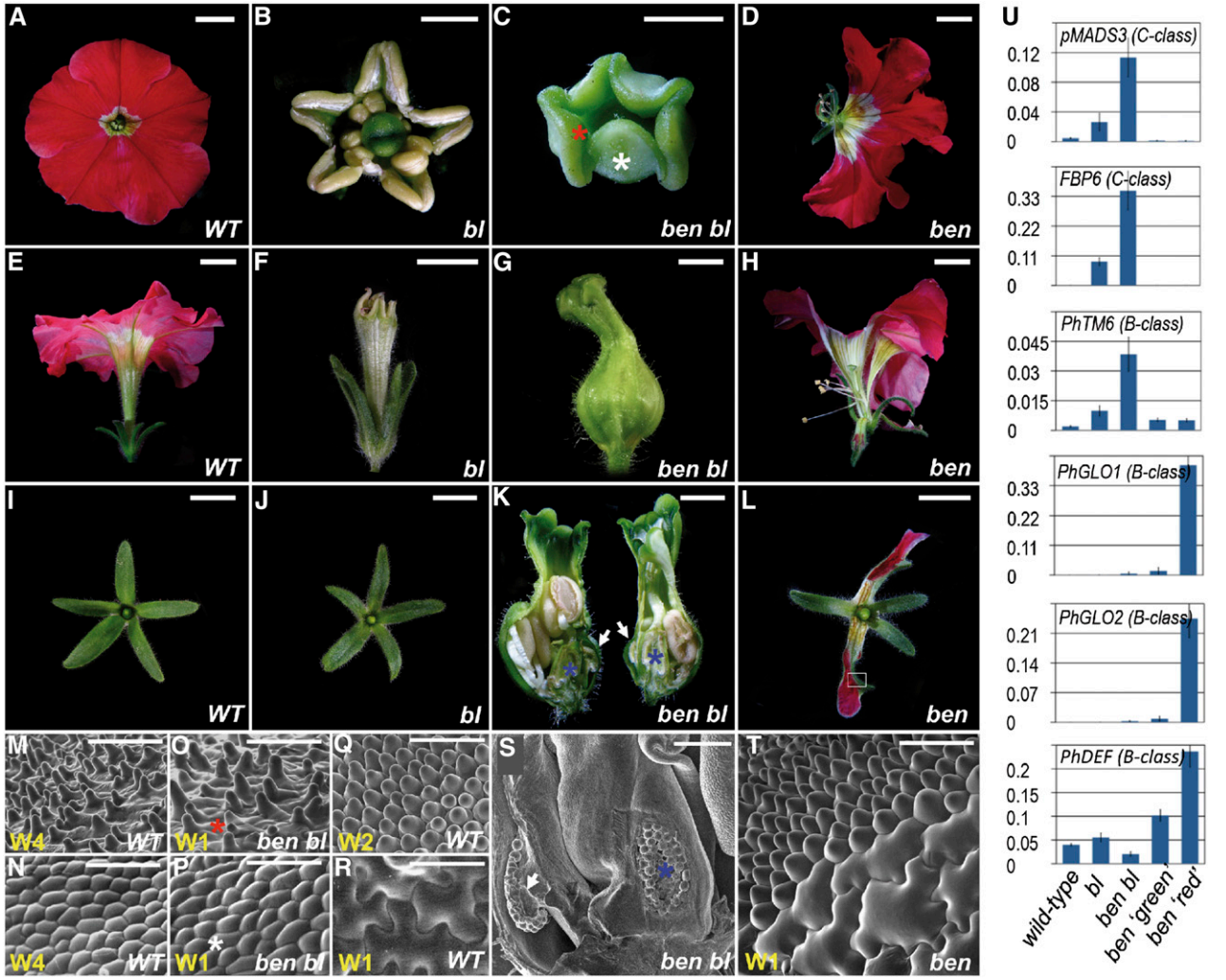

Figure 1. Floral and Molecular Phenotypes of Wild-Type, *bl*, *ben bl*, and *ben* Mutants

(A) to **(D)** Top view of entire flowers.
(E) to **(H)** Side view of entire flowers.
(I), **(J)**, and **(L)** Top view of dissected first whorl organs.
(K) Flower longitudinally sectioned. White arrows mark an ovary carrying ovules in the first whorl carpels.
(M) to **(T)** Scanning electron microscopy images of epidermal tissues of various floral organs in wild-type and mutants. Whorl numbers (W#) are marked in yellow. **(M)** and **(N)** correspond to wild-type stigma and ovary surfaces, respectively. Asterisks of the same color in different panels mark the correspondence of regions analyzed by scanning electron microscopy. The white rectangle in **(L)** marks the region analyzed by scanning electron microscopy in **(T)**, showing wild-type sepal epidermal cells in the green parts and conical petal cells in the colored parts. Bars = 1 cm, except 0.25 cm in **(B)**, **(C)**, **(G)**, and **(K)**, 50 μm in **(M)** to **(R)** and **(T)**, and 500 μm in **(S)**. Single and double mutants shown here are from alleles *bl-1* and *ben-488*.
(U) Relative expression levels of C- and B-class homeotic genes in stage 3 first whorl organs. *ben* 'green': green sepals; *ben* 'red': petaloid sepals. Data represent means ± SD of nine data points obtained from three biological replicates that each were analyzed in triplicate for qRT-PCR analysis. Relative expression (R.E.) values were normalized to the geometrical average of three reference genes. Biological replicates were obtained by pooling stage 3 first whorl organs from each time three different flowers.

B-function: In the large majority of the flowers, two opposing sepals oriented along the vertical flower axis were partially petaloid (Figure 1L), mimicking the color pattern of the wild-type petals, with the distal parts brightly colored as the corolla and a yellow/white pigmentation at their basis corresponding to the inner petal tube. At the cellular level, the pigmented regions displayed the typical conical cells found in the petal epidermis (Figures 1Q and 1T). The strength of the phenotype showed some variability, resulting in flowers on the same plant with sepals displaying petal sectors with variations in size, while a small minority of the flowers had either one or three sepals affected instead of two. This variability was observed to a comparable degree in all mutant individuals.

Finally, the majority of *ben* flowers displayed a corolla that is split open in one or two places, facing the homeotically converted sepals (Figures 1D and 1H). To further investigate the B-function patterning phenotype in these mutants, we monitored the expression of the three petunia B-class genes *DEFICIENS* (*DEF*), *GLOBOSA1* (*GLO1*), and *GLO2*, which in wild-type development specify petal identity in the 2nd whorl (Angenent et al., 1993; van der Krol et al., 1993; Vandenbussche et al., 2004). Not surprisingly, the expression levels of all three genes were dramatically increased in *ben* petaloid sepals compared with both wild-type sepals (Figure 1U) and *ben* sepals that did not display ectopic petal tissue. Compared with wild-type sepals, *DEF* expression also showed an increase in *ben* sepals that did not display petaloid sectors, but less dramatically. Remarkably, we observed no increase in *DEF*, *GLO1*, or *GLO2* expression in the *ben bl* mutants, indicating that the loss of *BL* function somehow antagonizes ectopic B-expression in the first whorl of *ben* mutants. We also analyzed the expression of petunia *TM6* (Rijpkema et al., 2006), an ancestral B-class gene that is present in many species but has been lost in Arabidopsis. In petunia, *TM6* acts a B-class gene to specify stamen development redundantly with *DEF* but is not involved in petal identity. Compared with wild-type sepals, *TM6* expression was enhanced in *bl* sepals, as reported earlier (Vandenbussche et al., 2004; Rijpkema et al., 2006), and increased further in *ben bl* sepals to a similar degree to the C-class genes. In contrast, only a very moderate increase was found in *ben* sepals. This is consistent with the finding that *TM6* expression largely depends on C-function activity (Heijmans et al., 2012), unlike classical B-class genes. Note that the ectopic *TM6* expression in *bl* and *ben bl* sepals does not lead to B-function activity in their sepals because TM6 requires PhGLO2 as an interaction partner to exert the B-function (Vandenbussche et al., 2004; Rijpkema et al., 2006), and *PhGLO2* is not ectopically expressed in *bl* and *ben bl* sepals (Figure 1U).

BEN Encodes a Member of the *AP2*/*ERF* Transcription Factor Family but Is Not Orthologous to the Arabidopsis A-Class *AP2* Gene

In a transposon display experiment (Van den Broeck et al., 1998; Vandenbussche et al., 2013) performed on selected progeny of the original family in which *ben* was segregating, we identified a single mutation induced by the transposon *dTph1* that fully cosegregated with the *ben* phenotype and found that *BEN* encodes a member of the *AP2*/*ERF* transcription factor family corresponding to the functionally uncharacterized *AP2B* gene (Maes et al., 2001) (Figure 2). Within the large *AP2*/*ERF* family, *AP2B* belongs to the *euAP2* lineage because of the combined presence of two AP2 domains and a miR172 target site (Kim et al., 2006). The *AP2B* gene consists of 10 exons (Figure 2C) with the *ben* allele containing a *dTph1* insertion positioned immediately after the first nucleotide of the third exon, 488 bp downstream of the ATG in the coding sequence (*ben-488* allele), disrupting the first DNA binding domain. Using *ben-488* primers flanking the putative insertion site (Supplemental Table 1), amplification and sequencing of *ben-488* transcripts revealed fragments considerably larger than the wild type (Figure 2A) containing the *dTph1* element but also the 2nd and 3rd introns, demonstrating that the incorporation of the *dTph1* element in the transcript affects splicing. This may be caused by the *dTph1*-induced 8-bp target site duplication, which includes the splice acceptor site of the 2nd intron and is duplicated immediately downstream of the *dTph1* element (Figure 2B).

To provide further independent genetic evidence that the *ben* phenotype is caused by the disruption of *AP2B* gene function, we screened our sequence-indexed *dTph1* transposon insertion collection (Vandenbussche et al., 2008) and identified two additional insertions in the *AP2B* coding sequence (Figure 2C), disrupting either the 2nd DNA binding domain (*ben-724*) or the first exon (*ben-139*). We found that flowers of *ben-724* and *ben-138* homozygous mutants display a very similar phenotype to that of *ben-488* as well as the offspring of an allelism test obtained by crossing *ben-488* and *ben-724* mutants (Figures 2E to 2J). In addition, we found that *ben-724 bl-2* double mutants exhibit a phenotype identical to that of the original *ben-488 bl-1* double mutants (Figures 2K and 2L). Given the insert positions of the three alleles in the coding sequence, and the finding that *dTph1* encodes stop codons in all six possible reading frames, we conclude that the phenotype observed in homozygous *ben* alleles is due to disruption of the *AP2B* gene and is most likely the result of a complete loss of function. To acknowledge its function, we renamed this gene *BEN.* The expression of *AP2B*/*BEN* was previously characterized by in situ hybridization, indicating a broad expression pattern, with transcripts detected in the bracts extending under the inflorescence meristems, in sepals, petals, stamens, and carpels, as well as in the endosperm of mature seeds (Maes et al., 2001). The results of qRT-PCR expression analysis (Figure 2D) are in agreement with these observations, and they show that *BEN* is already expressed in vegetative apices, albeit at lower levels compared with young flower buds, where expression peaks in stage 2 flowers (see Supplemental Figure 1 for stage definition). During later development (in stage 3 flowers, which have sufficiently developed to allow manual dissection of individual floral organs), *BEN* transcripts were detected in all floral whorls, but with highest expression in the carpels.

A sequence comparison with all six Arabidopsis *euAP2* genes (Supplemental Table 2) indicates that *RAP2.7* (*RELATED TO AP2.7*)/*TOE1* is the Arabidopsis gene most similar to *BEN*. *TOE1* was shown to act as a repressor of flowering (Aukerman and Sakai, 2003), but unlike *ben*, *toe1* mutants do not display defects in floral organ development. Conversely, we did not observe a flowering time phenotype in *ben* mutants. Because the function of *BEN* is more similar to that of the Arabidopsis *AP2* gene, this further suggests molecular divergence in the mechanisms that pattern the C-function between Arabidopsis and petunia.

Genome-Wide Phylogenetic Analysis of Petunia *euAP2* Genes

To better understand the relationship between *BEN* and the six different Arabidopsis *euAP2* genes, we took advantage of the recently released *Petunia axillaris* and *Petunia inflata* genome sequences (Bombarely et al., 2016) to compare all petunia and Arabidopsis *euAP2* genes in a phylogenetic analysis. *P. axillaris* and *P. inflata* species represent the main parents of modern *P. hybrida* varieties, including W138, the laboratory line used in

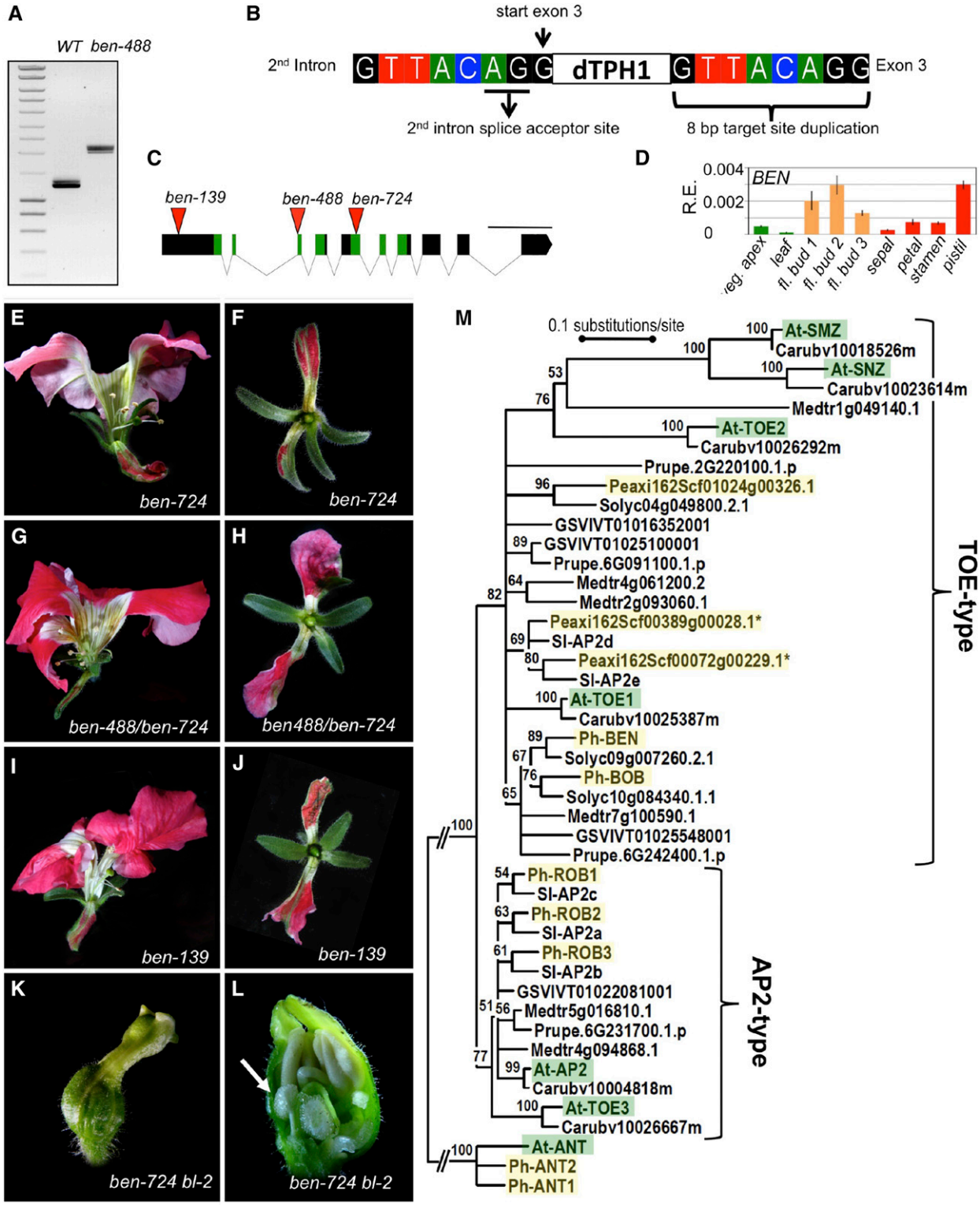

Figure 2. Molecular Characterization of *ben*.

(A) PCR amplification of *BEN* transcripts with primers *ben-488* (Supplemental Table 1) using flower bud cDNA templates from wild-type and *ben-488* plants, showing that *ben-488* transcripts are considerably larger than the wild type. *ben-488* corresponds to the *dTph1* insertion allele identified in the transposon display experiment (see Methods).

this study. We identified eight predicted *euAP2* proteins in *P. axillaris*, while nine were detected in *P. inflata*. Comparison between the two species showed that the extra *euAP2* gene copy in *P. inflata* is due to a recent duplication of one of the eight genes (Supplemental Table 3 and Supplemental Figure 2A). Representatives of five out of the eight *P. axillaris*/*P. inflata* gene pairs were experimentally confirmed in W138 and further analyzed in this study (Supplemental Table 3), including the previously described *P. hybrida AP2B* (*BEN*) and *AP2A* genes. We retained the five W138 *euAP2* genes and three remaining *P. axillaris* representatives to be included in the phylogenetic analysis. Furthermore, we also included the *euAP2* genes (Supplemental Table 3) from *Capsella rubella* (Slotte et al., 2013), a Brassicaceae species closely related to Arabidopsis, the asterid species tomato (*Solanum lycopersicum*; Tomato Genome Consortium, 2012) as a close relative of petunia, and the species *Medicago truncatula* (Young et al., 2011), *Vitis vinifera* (grape) (Jaillon et al., 2007), and *Prunus persica* (peach) (Verde et al., 2013), all rosid species distant from Arabidopsis and from each other. In agreement with a recent phylogenetic analysis (Wang et al., 2016), we found that all *euAP2* sequences cluster in either of two different groups with well-supported bootstrap values, corresponding to TOE and AP2 types (Figure 2M). Furthermore, orthologous relationships are well supported between *euAP2* genes from closely related species, showing six pairs of Arabidopsis/*C. rubella* genes and eight pairs of petunia/tomato genes. In line with the sequence comparison (Supplemental Table 2 and Supplemental Figure 2B), the phylogenetic analysis indicates that *BEN* is more closely related to *TOE1* than to *AP2*. Within the TOE-type group, however, the aligned region on which the tree is based does not provide enough resolution to completely resolve relationships between members from distantly related species, but the divergent TOE2 and SMZ/SNZ clades (Wang et al., 2016) can be clearly distinguished. Petunia possesses in total five *euAP2* genes that belong to the TOE-type, with one gene similar to *BEN* (see next paragraph) and three other genes that are more distantly related. Finally, petunia harbors three *euAP2* genes that belong to the AP2-type class (see further).

BOB and *BEN* Are Redundantly Required for Proper Development of Second and Third Whorls

We hypothesized that the subtle B-function patterning defects found in *ben* single mutants might represent the first signs of an unknown major mechanism that prevents B-class expression in the petunia sepals, encoded by *BEN* in a largely redundant fashion with one or more unknown factors. We found that petunia contains a gene closely related to *BEN* (Figure 2M; Supplemental Figures 2A and 2B), which we named *BOB* (for *BROTHER OF BEN*). Because *BOB* expression overlaps with *BEN* in all tissues tested (Figure 3A), we selected *BOB* as a plausible candidate to encode a B-repression function in sepals, redundantly with *BEN*.

We applied a reverse genetics approach to test this and identified two putative null mutations, *bob-213* and *bob-519* (Figure 3B), but homozygous mutants were not different from the wild type (Figures 3C, 3D, 3G, and 3H), suggesting full redundancy. We therefore tested a putative functional overlap with *BEN* by analyzing *ben bob* double mutants. We found that in all *ben bob* flowers (Figures 3E and 3F), 2nd whorl petal development was strongly reduced. This phenotype ranged from flowers in which all five petals appeared to be absent (Figure 3E) to flowers in which one or more petals developed but were always strongly reduced in size (Figure 3F). No signs of homeotic conversions were observed in these 2nd whorl petals. In the third whorl, most flowers contained fewer than five stamens, some of which occasionally fused entirely with the remnants of the 2nd whorl petals. The central pistil appeared normal. These observations indicate that *BEN* and *BOB* are redundantly required for proper 2nd and 3rd whorl development, a phenotype reminiscent of strong Arabidopsis *ap2* alleles, which also display similar growth defects in these whorls. Despite this strong phenotype, the first whorl sepals of the double mutants were undistinguishable from those of *ben*

Figure 2. (continued).

(B) Sequencing of *ben-488* transcripts revealed a *dTph1* transposon cotranscribed in the transcript and inserted directly after the first nucleotide of exon 3, followed by an 8-bp target site duplication, which duplicates the 2nd intron splice acceptor site.

(C) *BEN* genomic structure (from start to stop codon) showing the positions of additional independent *dTph1* transposon insertions (red triangles). Rectangles and lines represent exons and introns, respectively. Green regions indicate the two AP2 domains. Numbers in allele names correspond to insert positions (expressed in base pairs) downstream of the ATG in the coding sequence. Bar = 500 bp.

(D) Expression levels of *BEN* transcripts in different wild-type tissues. Data represent means ± SD of nine data points obtained from three biological replicates that each were analyzed in triplicate for qRT-PCR analysis. Relative expression (R.E.) values were normalized to the geometrical average of three reference genes. Green bars, vegetative tissues; orange bars, complete floral buds from stage 1, diameter 1.5 mm; stage 2, diameter 2.5 mm; and stage 3, diameter 5 mm. Red bars indicate individual organs dissected from stage 3 (see Supplemental Figure 1 for floral stage definition and Methods for sample description).

(E) to **(L)** Phenotypes of additional *ben* alleles and crosses. Flowers of *ben-724*, *ben-138*, and *ben-488*/*ben-724* mutants display phenotypes very similar to *ben-488*. In addition, *ben-724 bl-2* double mutants exhibit a phenotype identical to *ben-488 bl-1* double mutants (compare with Figure 1).

(E), **(G)**, **(I)**, and **(K)** Side views of undissected flowers.

(F), **(H)**, and **(J)** Top view of first whorl organs.

(L) Longitudinal flower section showing inner organization. The white arrow indicates a placenta with ovules in the first whorl.

(M) Neighbor-joining tree of euAP2 proteins from petunia (Ph; Peaxi, shaded in yellow), tomato (Sl; Sol), Arabidopsis (At, shaded in green), *C. rubella* (Carub), *M. trunculata* (Medtr), grape (GSVIV), and peach (Prupe), rooted with AINTEGUMENTA (ANT) proteins. Bootstrap values (%) based on 2000 replicates are indicated near the branching points; branches below 50% have been collapsed.

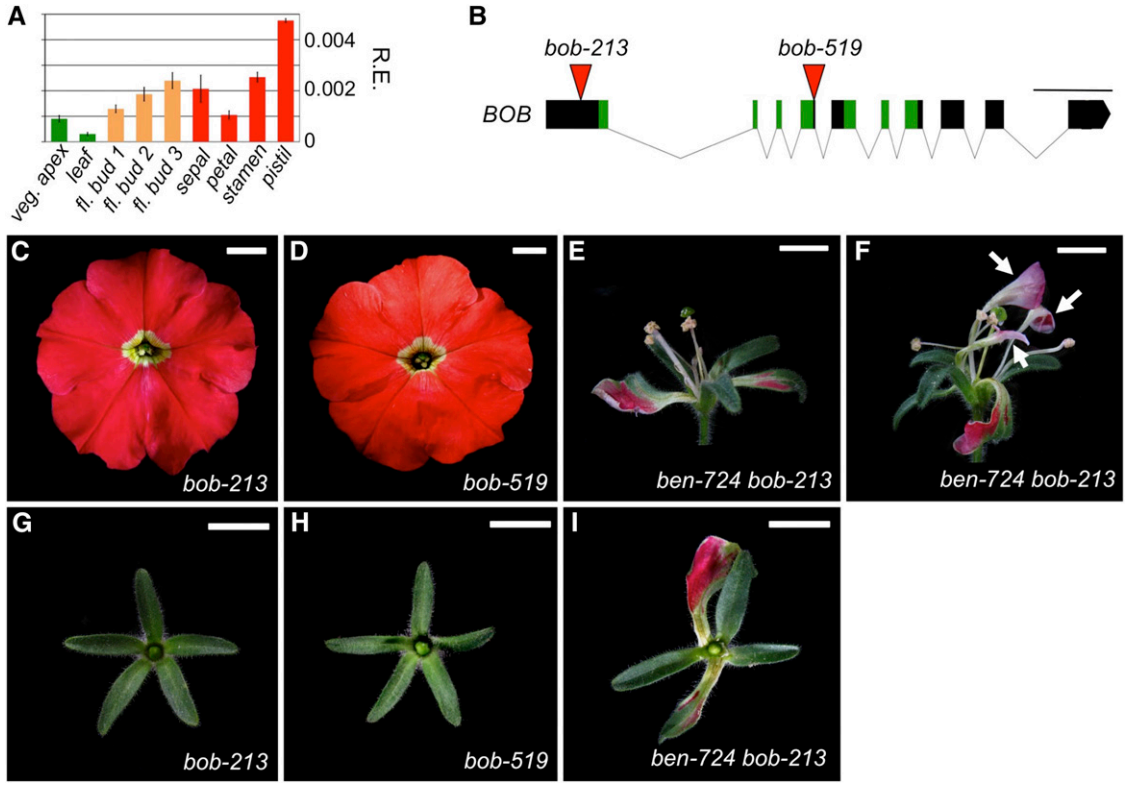

Figure 3. Characterization of Petunia *BOB* and Genetic Interactions with *BEN*.

(A) Expression levels of *BOB* transcripts in different wild-type tissues. *BOB* expression overlaps with *BEN* expression in all tissues tested, showing the highest expression levels in carpels of stage 3 flowers. Legend and cDNA templates as in Figure 2D.
(B) *BOB* genomic structure and position of *dTph1* transposon insertions. Legend as in Figure 2C.
(C) to **(I)** Floral phenotypes of *bob* and *ben bob* mutants showing complete flowers in **(C)** to **(F)** and dissected first whorls in **(G)** to **(I)**. **(C)**, **(D)**, **(G)**, and **(H)** are homozygous *bob* mutants display a wild-type floral architecture, suggesting redundancy. Bars = 1 cm.
(E) and **(F)** *ben bob* flowers display severe 2nd whorl growth defects.
(E) Flower completely lacking petals.
(F) Flower with strongly reduced petals (white arrows). In addition, one to two stamens are often missing in the third floral whorl.
(I) *ben bob* first whorl organs are similar to those of *ben*.

single mutants (Figure 3I), indicating that *BOB*, in contrast to *BEN*, most likely is not involved in patterning the B-function.

Petunia *ROB1*, *ROB2*, and *ROB3* AP2-Type Genes Are Required for Proper Perianth and Pistil Development, but Do Not Antagonize the C-Function in the Outer Whorls

Because the petunia equivalent of the Arabidopsis *AP2*-mediated C-patterning function is encoded by *BEN*, which belongs to the *TOE*-type class, the function of the petunia *AP2*-type members remained to be determined. Exploring the petunia genomes (Bombarely et al., 2016), we found that in addition to the previously reported *AP2A* gene (Maes et al., 2001), petunia contains two additional AP2-type genes (Figure 2M; Supplemental Figures 2A and 2B). We named these additional genes *ROB2* and *ROB3* (for *REPRESSOR OF B-FUNCTION*, for reasons explained later), while petunia *AP2A* was renamed *ROB1* (Figure 2M). While the phylogenetic analysis within the AP2-type group only provides moderate support (bootstrap value of 51%) for grouping the petunia *ROB* genes with Arabidopsis *AP2*, a global sequence comparison with all six Arabidopsis *euAP2* genes indicates that *AP2* is the Arabidopsis gene most similar *to ROB1*, *-2*, and *-3* (Supplemental Table 2 and Supplemental Figure 2B). Expression of *ROB1* (*AP2A*) during floral development was previously characterized by in situ hybridization, indicating comparable expression levels in all four floral whorls during early floral stages, while later on, its expression appeared to be stronger in petals and the ovary compared with the other floral organs (Maes et al., 2001). In addition, transcripts were also detected in seeds and in leaf primordia of young seedlings.

By qRT-PCR analysis (Figure 4A), we found that the three *ROB* genes display broad and quite comparable expression patterns, showing the highest expression levels in petals and carpels in stage 3 flowers, while also being well expressed in vegetative tissues. Given these overlapping expression patterns, the absence of an Arabidopsis *ap2*-like phenotype in the reported petunia *ap2a* mutants might also be simply explained by a putative redundancy with *ROB2* and *ROB3*. Therefore, it could not yet be excluded that petunia *AP2*-type genes function

in a similar manner to Arabidopsis *AP2*. To test this hypothesis, we analyzed the function of the three *ROB* genes. For all three genes, we identified and confirmed candidate *dTph1* insertions in the coding sequence (Figure 4B), positioned either in the first exon (in the case of *ROB1*) or disrupting the highly conserved 2nd AP2 domain (for *ROB2* and *ROB3*). Homozygous *rob1* mutant flowers were not different from the wild type, confirming previous results (Maes et al., 2001), nor were the flowers of *rob2* and *rob3* mutants (Supplemental Figure 3), suggesting redundancy for all three *ROB* genes. To test this, we analyzed genetic interactions between the different *rob* mutants. Our results indicate that all three *ROB* genes function in a largely redundant fashion, since double mutants only displayed subtle phenotypes if any at all (Supplemental Figure 3), while a clearly recognizable and uniform phenotype different from the wild type was observed in all flowers of triple *rob1 rob2 rob3* mutants. We found that *rob1 rob2 rob3* petal lobes were less developed, resulting in a more star-like shaped corolla compared with the round petal lobes found in wild-type flowers (Figures 4C and 4E). In addition, triple mutant petals displayed an altered pigmentation, colored pink rather than the bright red color found in the wild type. These pale-pink flowers were exclusively found in all triple homozygous mutants, but colors intermediate between the wild type and the triple mutant were found in some double mutant combinations (Supplemental Figures 3F and 3G), indicating that petunia *ROB* genes apparently contribute to petal pigmentation in a redundant but additive fashion. Furthermore, we found that the length of the pistil was always reduced in triple mutants compared with the wild type, mainly due to a reduction in style length, while stamen development was not affected (Figure 4F). In addition, the sepals of early arising *rob1 rob2 rob3* flowers (Figure 4G) were larger compared with the wild type (Figure 1I) and lower order mutants (Supplemental Figure 3I), but this difference became much less pronounced in flowers developing later (Supplemental Figure 3J).

In summary, no morphological indications of C-patterning defects in the perianth organs were found, in sharp contrast to *ap2* mutants in Arabidopsis. This was also confirmed at the molecular level, showing that the expression of the two petunia C-class genes *pMADS3* and *FBP6* remain restricted to the stamens and carpels, as in the wild type (Figure 4J). This demonstrates that *ROB* genes are not required to repress the C-function in sepals and petals. Yet, it was still possible that they would function as C-repressors in the perianth but that this function is masked by *BL*, similar to what was found earlier for *BEN*, whose C-repressor role was only revealed in a *bl* mutant background. To answer this question, we created and analyzed *bl rob1 rob2 rob3* quadruple mutants. In contrast to *bl ben*, flowers of these quadruple mutants were not markedly different from those of *bl* mutants (compared with Figures 4H, 1F, and 1G), except for the sepals of early arising flowers (Figure 4I), which were larger, similar to those observed in early arising *rob1 rob2 rob3* flowers. Based on these results and the phenotypes of *rob* lower order mutant combinations, we conclude that the *ROB* genes are redundantly required for normal development of sepals, petals, and carpels, but are unlikely to antagonize the C-function in the perianth.

BEN, *ROB1*, *ROB2*, and *ROB3* Genes Redundantly Repress the B-Function in Sepals

Intriguingly, we noticed that the first two to three flowers that appeared on the inflorescence of triple *rob* and quadruple *rob bl* mutants displayed sepals that were not only larger, but in addition contained petaloid regions found primarily at the base of the sepal margins (Figures 4G and 4I). This phenotype was clearly observed in around half of these early flowers. This indicated that patterning of the B-function genes is partially impaired, as also observed in *ben* single mutants. This phenotype was not seen in lower order mutants and disappeared completely in later arising flowers in *rob1 rob2 rob3* (*bl*) mutants (Supplemental Figures 3I to 3K). Earlier, we hypothesized the existence of a novel major mechanism in petunia that prevents B-class expression in the sepals, encoded by *BEN* in a largely redundant fashion with one or more other unknown factors. Although being the most obvious candidate, we failed to show such a common B-repressor function for *BOB*, the closest relative of *BEN*. Interestingly, although the *ROB* genes are more distantly related to *BEN* than *BOB*, the subtle B-function patterning defect observed in the triple *rob* mutant flowers identified the *ROB* genes as other possible candidates to repress the B-function together with *BEN*. To test this, we analyzed genetic interactions of *ben* with the *rob* mutations.

To our delight, we found that all flowers of *ben rob1 rob2*, *ben rob1 rob2 rob3*/+, and *ben rob1 rob2 rob3* mutant individuals displayed a quasi-complete homeotic transformation of their sepals into petals, which as in 2nd whorl wild-type flowers were fully fused, forming a tube and corolla with a size close to the wild type (Figures 5A to 5J). No obvious morphological differences were found between *ben rob1 rob2* and *ben rob1 rob2 rob3*/+ flowers, while quadruple mutant flowers could be clearly distinguished based on the pink color of their petals and the more star-like shape of the corolla, as found earlier in the 2nd whorl of triple *rob* mutants.

Outgrowth of the 2nd whorl petals in all flowers of *ben rob1 rob2*[*rob3(/+)*] mutants was affected, but to a variable degree, with phenotypes ranging from a 2nd whorl being (almost) completely absent (Supplemental Figures 3L, 3M, and 3O) to flowers with five well-developed petals, but always with fusion defects between one or more petals (Figures 5C and 5D). Finally, the completeness of sepal to petal conversion varied slightly between flowers on the same plant, ranging from first whorl petals that retained some partial sepal-like characteristics, as indicated by a green hue, mainly around the central petal veins, to flowers in which conversion appeared complete in all five first whorl petals (compared with Supplemental Figures 3N and 3O). These variable aspects of the phenotype were observed to a comparable degree in all *ben rob1 rob2* [*rob3(/+)*] mutant individuals. While petunia wild-type sepals do not senesce after fertilization, *ben rob1 rob2* [*rob3(/+)*] first whorl petals wilt in a similar manner to wild-type petals (Figures 5F and 5J). Consistent with the quasi-complete conversion of sepals into petals in these mutants, we found that the petunia B-function genes reach expression levels in the first whorl comparable to those normally observed in wild-type 2nd whorl petals (Figure 5K). In situ hybridization (Figure 5L) further revealed that ectopic B-expression in the petaloid first whorl organs already occurs at the very early stages of floral development, when first whorl primordia start to arise from the floral meristem. Similar to triple *rob1 rob2 rob3* mutants, we did not find upregulation of the C-genes in the first whorl of *ben rob1 rob2 rob3* mutants compared with wild-type sepals (Figure 5K). Together, we conclude that the *ROB* genes pattern the B-function genes (but not the C-function genes) by acting as repressors of the B-function in the first floral whorl, redundantly with *BEN*. For this reason, we have (re)baptized *AP2A* and the two other AP2-type

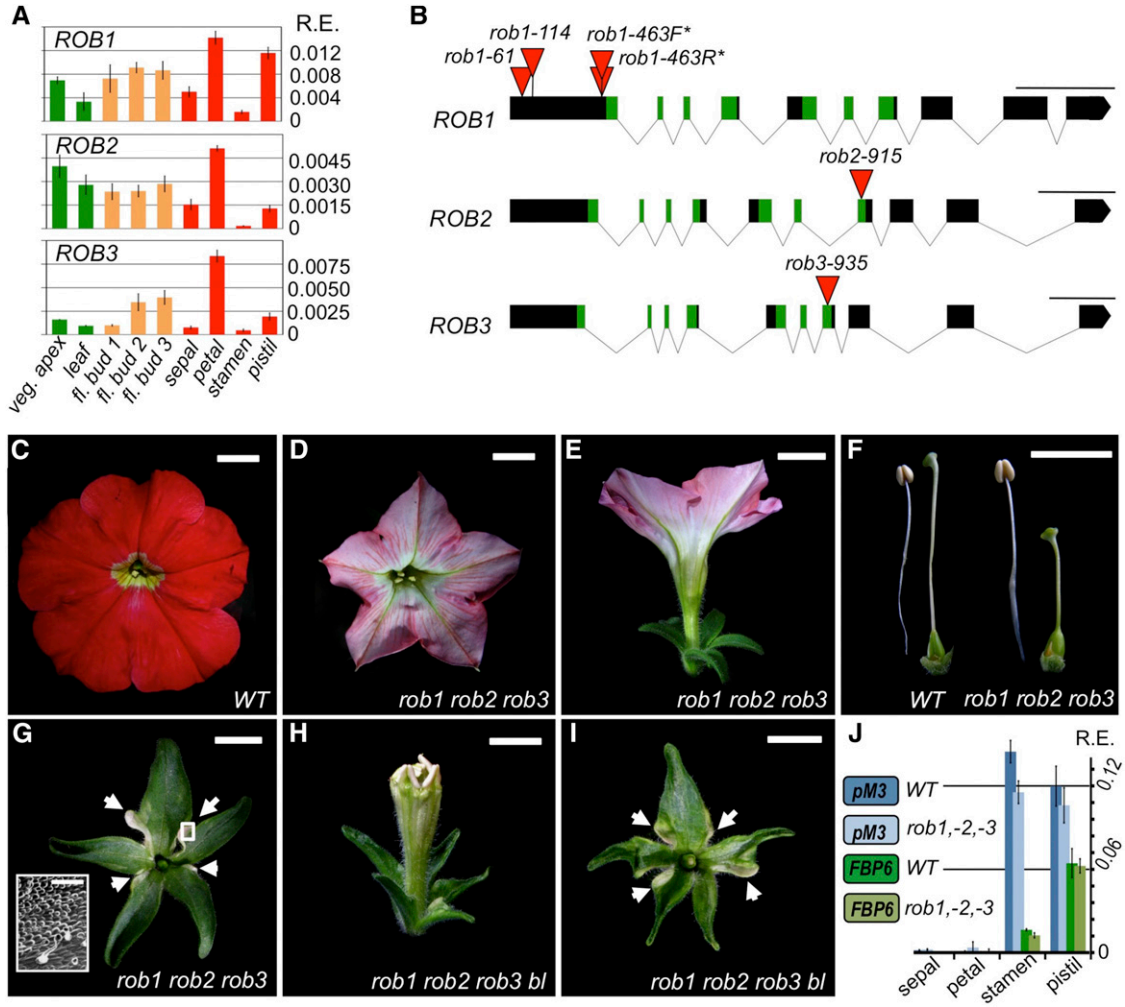

Figure 4. *ROB* Genes Are Redundantly Required for Normal Sepal, Petal, and Carpel Development but Do Not Antagonize the C-Function in the Perianth.

(A) Expression levels of *ROB* genes in different wild-type tissues. The petunia *ROB* genes are widely expressed and show very similar expression patterns. Legend and cDNA templates as in Figure 2D.

(B) Genomic structures and positions of *dTph1* transposon insertions identified in the petunia *ROB* genes. Note that *rob1-463F* and *rob1-463R* are two independent insertions at the same position, but with opposite orientations of the *dTph1* transposon. Legend as in Figure 2C.

(C) to **(E)** and **(H)** Undissected flowers.

(F) Comparison of stamens and pistils.

(G) and **(I)** First whorl organs. White arrows indicate petaloid regions. Inset in **(G)**: scanning electron microscopy analysis showing conical petal cells in the region indicated by the rectangle in **(G)**.

(J) qRT-PCR analysis of C-class MADS-box gene expression in different floral organs (stage 3), showing a similar expression pattern in wild-type and *rob1 rob2 rob3* mutants. Data represent means ± SD of nine data points obtained from three biological replicates that each were analyzed in triplicate for qRT-PCR analysis. Relative expression (R.E.) values were normalized to the geometrical average of three reference genes. Biological replicates were obtained by pooling organs from each time three different flowers. Mutants shown here were made using *rob1-61*, *rob2-915*, *rob3-935*, and *bl-2* insertion alleles. Bars = 1 cm, except for inset in **(G)** where bar = 100 μm.

genes with the names *ROB1*, *ROB2*, and *ROB3*, for *REPRESSOR OF B-FUNCTION.*

A Combinatorial Model for Patterning the Floral Homeotic B- and C-Functions in Petunia Flowers

We have summarized our findings thus far in a combinatorial model describing the patterning of the floral homeotic B- and C-functions during petunia flower development (Figure 6A). Note that for clarity, the presented model has been simplified at different levels: (1) The expression domains of the genes regulating the B- and C-functions are not necessarily restricted to the first two whorls. What is shown in the model is rather the final outcome of their action on the patterning of the B- and C-genes in the perianth. For example, *BL*, like its ortholog *FIS* in snapdragon, is expressed in all floral whorls and is proposed to pattern the C-genes by

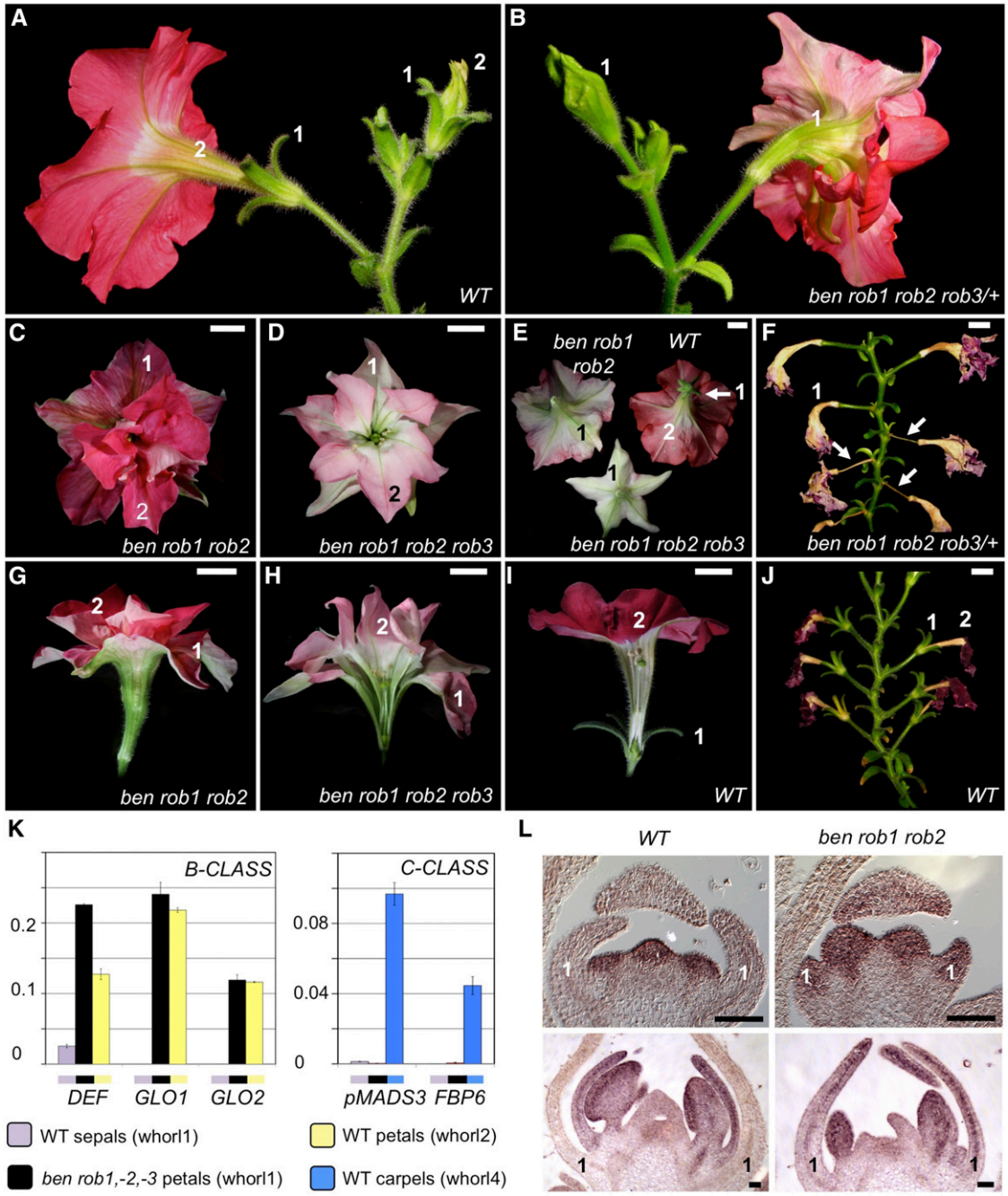

Figure 5. *BEN* and *ROB* Genes Repress the B-Function in the First Whorl.

(A) and **(B)** Inflorescences showing flowers at various stages of development. "1" and "2" indicate whorl numbers in **(A)** to **(L)**.
(C) and **(D)** Top view of *ben rob* flowers.
(E) Bottom view.
(G) to **(I)** Side views; flowers in **(H)** and **(I)** have been sectioned to reveal inner organization.
(F) and **(J)** Inflorescences shown from first wilted flower downwards. Mutants shown here were made using *rob1-61*, *rob2-915*, *rob3-935*, *ben-724*, and *bl-2* insertion alleles.
(K) qRT-PCR analysis of B- and C-function genes in individual floral organs (stage 3). Data represent means ± SD of nine data points obtained from three biological replicates that each were analyzed in triplicate for qRT-PCR analysis. Relative expression (R.E.) values were normalized to the geometrical average of three reference genes. Biological replicates were obtained by pooling organs from each time three different flowers. The B-class genes *DEF*, *GLO1*, and *GLO2* are strongly upregulated in *ben rob1 rob2 rob3* first whorl petals compared with first whorl wild-type sepals, reaching expression levels

dampening the expression of the C-genes within their genuine expression domain in the center of the flower, thereby preventing outward spreading of the C-function into the perianth (Cartolano et al., 2007). (2) The petunia B- and C-functions, although fully characterized (Vandenbussche et al., 2004; Rijpkema et al., 2006; Heijmans et al., 2012), are not shown in detail. The petunia B-function in particular is more complex compared with Arabidopsis and snapdragon, mainly due to the presence and atypical features of *TM6* (Rijpkema et al., 2006). (3) Because the B-patterning function is encoded by *BEN* and the *ROB* genes in a largely redundant fashion, no individual graphs are shown for single *ben* or triple *rob* mutants.

In this model, C-function repression in the perianth is controlled by two parallel pathways, with *BL*-mediated repression as the dominant mechanism, while *BEN* fulfills a secondary role by preventing C-function activity in the first whorl in the absence of *BL*. When *BL* is functional, *BEN* acts together with the *ROB* genes as major B-function repressors in the first whorl. One of the attractive features of the classical ABC model is, besides the beauty of its simplicity, the possibility to predict the outcome of higher order mutant combinations. Interestingly, our model predicts the development of stamens in the first whorl in a *bl ben rob* mutant background (Figure 6A, red arrow) due to the predicted simultaneous expression of B- and C-functions in the first whorl. However, full stamen identity may require a well-balanced B/C coexpression. To test this, we combined *ben*, *bl*, and *rob* mutations together and found that stamen/antheroid structures indeed developed in the first whorl of *ben bl rob1 rob2 rob3(/+)* flowers, in line with the model's prediction. In the majority of the flowers, two to three first whorl organs could be observed that macroscopically resembled wild-type anthers (Figures 6B, 6G, and 6H) as well as at the cellular level (Figure 6E and 6F), while the remaining organs were more carpelloid as in *bl ben* mutants. Occasionally, we found flowers in which first whorl anthers were supported by a stamen filament as in the wild type (Figure 6C). Much more rarely (in three cases only), we observed flowers in which all first organs appeared antheroid (Figure 6D).

DISCUSSION

Divergent Mechanisms Antagonizing the C-Function in the Perianth of Petunia and Arabidopsis

During the last two decades, the classic ABC model of floral development (Bowman et al., 1991; Coen and Meyerowitz, 1991) has been used with great success as an evolutionary genetic framework to study floral development and diversity. However, extending the molecular basis of the Arabidopsis A-function to other eudicot species has largely failed thus far. Note that a snapdragon A-function was originally postulated based on a semidominant mutation, called *ovulata*, but was later shown to be the consequence of a gain-of-function mutation in the C class gene *PLENA* (Bradley et al., 1993). Later on, forward genetic screens in petunia and snapdragon revealed a completely different molecular mechanism encoding the major factor preventing C-expression in the perianth: the *miR-BL/FIS-NF-YA* module in petunia and snapdragon (Cartolano et al., 2007), compared with *AP2*-mediated C-patterning in Arabidopsis (Kunst et al., 1989; Bowman et al., 1991; Drews et al., 1991; Jofuku et al., 1994; Dinh et al., 2012). Yet *AP2* orthologs exist in petunia and snapdragon, and all components of the *miR-BL/FIS* (*miR169*) module are present in Arabidopsis (Mantovani, 1999; Hong et al., 2003; Jones-Rhoades and Bartel, 2004). In theory, it is therefore possible that *AP2* and *miR-BL/miR169* modules in both species act in parallel to pattern the C-function. However, even if *miR169* in Arabidopsis and *AP2* orthologs in petunia/snapdragon would play a role in C-patterning, they clearly cannot compensate for the loss of *AP2* and *BL/FIS* function, respectively, indicating that the two species have retained different mechanisms representing the major regulator to repress the C-function in the perianth. Because the *bl/fis* mutants display only an incomplete C-patterning defect (their first whorl organs retain sepal identity), this suggested that one or more additional factors may exist that repress the C-function together with *BL/FIS*. Here, we have shown that *BEN* represents such a factor: The *ben* mutation strongly upregulates ectopic C-gene expression in the first whorl of *bl* mutants, leading to the full homeotic conversion of sepals into carpels and resulting in a *ben bl* floral phenotype closely resembling the strongest *ap2* alleles in Arabidopsis. The observation that *BEN*'s C-repressor function only becomes visible in a *bl* mutant background further supports the idea that the *BL* function represents the dominant C-patterning mechanism in petunia. Although *BEN* appears to encode the functional equivalent of Arabidopsis *AP2*, *BEN* is more similar to Arabidopsis *TOE1*. No floral patterning defects thus far have been described for *toe1* mutants: Gain- and loss-of-function analyses showed that *TOE1* acts as a floral repressor (Aukerman and Sakai, 2003). In turn, we found that the *ROB* genes, the petunia *euAP2* genes with highest similarity to Arabidopsis *AP2*, are redundantly required for normal development of sepals, petals, and the ovary but do not antagonize the C-function in the perianth. This is similar to what has been previously described for the snapdragon *AP2* homologs *LIP1/LIP2* (Keck et al., 2003).

Antagonism of the B-Function in the First Floral Whorl

Inspired by subtle B-function patterning defects commonly found in *ben* and *rob1 rob2 rob3* mutants, we discovered a floral patterning mechanism in petunia flower development, encoded by *BEN* and *ROB* genes, that prevents B-function expression in the

Figure 5. (continued).

comparable to those observed in wild-type 2nd whorl petals. The C-class genes *pMADS3* and *FBP6* are expressed at very low levels in sepals compared with carpels in the wild type and remain expressed at very low levels in *ben rob1 rob2 rob3* first whorl petals.

(L) In situ hybridization of *PhGLO2* in wild-type and *ben rob1 rob2* mutants at early stages of development, showing ectopic *PhGLO2* expression in first whorl primordia of *ben rob1 rob2* flowers. First floral whorls (1) are indicated. Bars = 1 cm, except in **(L)** where bar = 50 μm.

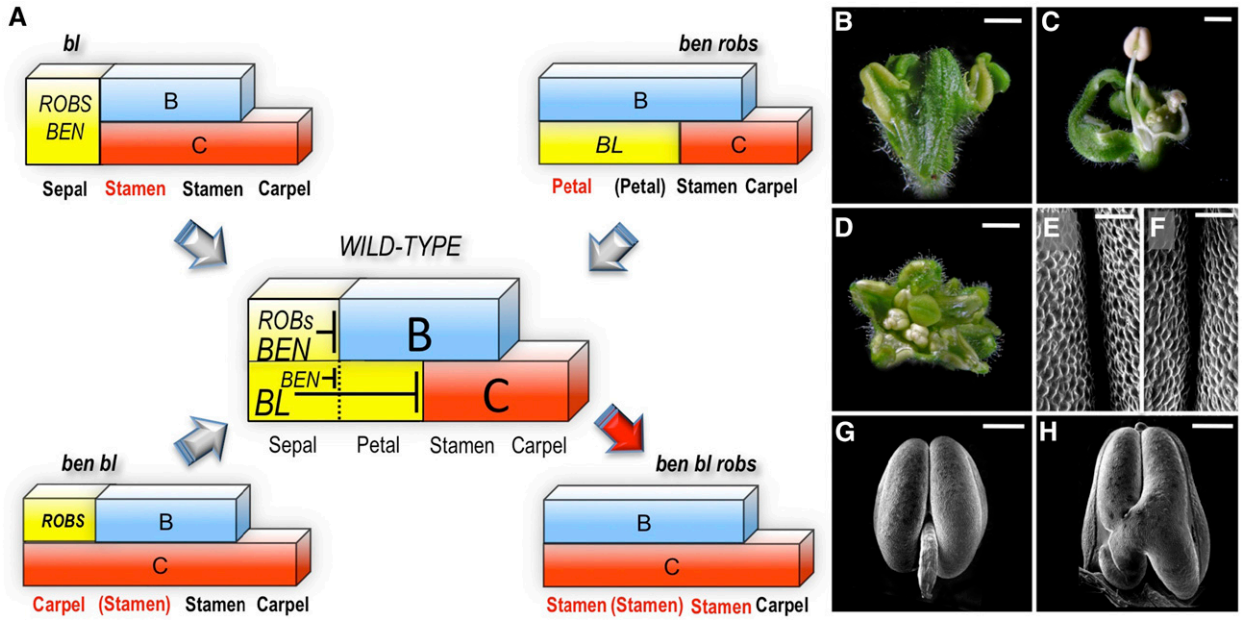

Figure 6. A Simplified Combinatorial Model Describing the Cadastral (Boundary Setting) Functions That Pattern the Floral B- and C-Functions in Petunia.

(A) The yellow block in the wild type represents combinatorial repression of the petunia B- and C-functions in sepals and the C-function in petals. The model is based on floral phenotypes and genetic interactions of three classes of homeotic mutants (*bl*, *ben bl*, and *ben rob1-3*) described in this study and predicts stamen development in the first whorl in a *ben bl robs* mutant background (red arrow). See main text for additional information.
(B) and **(C)** Side view of *ben bl rob1 rob2 rob3*/+ flowers showing stamens and antheroid structures in the first whorl, respectively.
(D) Top view of a *ben bl rob1 rob2 rob3* quintuple mutant showing antheroid organs in the first whorl.
(E) to **(H)** Scanning electron microscopy images of third whorl anthers (**[E]** and **[G]**) and of first whorl antheroids observed in *ben bl rob1 rob2 rob3*/+ flowers (**[F]** and **[H]**). Bars = 2 mm in **(B)** to **(D)**, 50 μm in **(E)** and **(F)**, and 200 μm in **(G)** and **(H)**.

first floral whorl. Remarkably, the petals developing in the first whorl of *ben rob1 rob2* (*rob3*) flowers closely resemble wild-type 2nd whorl petals, displaying complete fusion and proper tube and corolla development. Compared with this phenotype, the B-patterning defects observed in single *ben* and triple *rob* mutants are very subtle, indicating that *BEN* and the *ROB* genes repress the B-function in the first floral whorl in a largely redundant way. Nevertheless, these phenotypes indicate that *BEN* function is more critical in the sepals along the vertical floral axis compared with the lateral sepals, while *ROB* gene function might be more critical in early arising flowers. A complete homeotic conversion of all sepals into petals and in all flowers produced throughout development as observed in *ben rob1 rob2* (*rob3*) flowers never has been reported in Arabidopsis through loss-of-function mutations. Homeotic patterning defects in strong Arabidopsis *ap2* alleles only affect the C-function expression domain (Kunst et al., 1989; Bowman et al., 1991), indicating that the primary patterning function of *AP2* is to restrict the C-function to the inner floral whorls. However, there is evidence that *AP2*, besides its role in C-repression, also prevents B-expression in the sepals: First, some *ap2* alleles were reported to contain mosaic organs consisting of carpel and stamen sectors in the medial positions of the first whorl, which is indicative of local simultaneous *B*- and *C*-class gene expression (Bowman et al., 1991). More recently, it was found that introducing the *ap2-2* mutation in a heterozygous state in the dominant-negative *tpl-1* (*topless-1*) mutant enhanced the frequency of flowers displaying petaloid sepals compared with *tpl-1* mutants (Krogan et al., 2012). Although why these B-patterning defects only become apparent in specific *ap2* alleles and/or genetic backgrounds is not well understood, this provided clear genetic support for a model in which *AP2*, in addition to repressing the C-function gene *AG*, also regulates the expression borders of the B- and E-class genes by recruiting TPL and the histone deacetylase HDA19 (Krogan et al., 2012).

Combined Ectopic Expression of the Homeotic B- and C-Functions in the First Whorl?

Single *ben* mutants display a partial but clear B-patterning defect in the first whorl, while intriguingly, *ben bl* mutants only show an enhanced C-function patterning defect in their first whorl organs (Figure 1). Because *BL* is a negative regulator of *NF-YA* genes, which are proposed to act as positive regulators of C-gene expression, a lack of ectopic NF-YA activity in *ben* single mutants may explain why the loss of *BEN* alone is not sufficient to activate ectopic C-activity in the perianth. Therefore, although *BEN* patterns both the B-and C-functions, only the B-function expression domain is affected in *ben* single mutants. On the other hand, it is less obvious why *ben bl* mutants do not show simultaneous B- and C-function activity in the first whorl, at least in two out of the five first whorl organs, as would normally be expected based on the

combination of the single mutant phenotypes (Figure 1). On the other hand, combined B- and C- activity does occur in the first whorl of *bl rob1 rob2 rob3(/+)* mutants, as indicated by the presence of antheroid organs (Figure 6). Because the *ROB* genes still partially repress the B-function in the first whorl of *ben* mutants (and *ben bl* mutants), this may suggest that ectopic C-function gene expression may have a strong negative impact on the expression level of the B-function genes, in a context in which B-function repression is only partially impaired. In other words, this suggests that the establishment and/or upregulation and further maintenance of the C- and B-function expression domains may not be fully independent. At the moment, we can only speculate how this occurs in petunia, and direct or indirect interactions are equally possible. Interestingly, in Arabidopsis, both B- and C-class MADS-box proteins require complex formation with SEPALLATA (SEP) proteins for their positive autoregulation (Gómez-Mena et al., 2005; Kaufmann et al., 2009). Thus, B- and C-function proteins compete for the same substrate (SEP3) required for further upregulation and maintenance. According to the quartet model (Theissen and Saedler, 2001), carpel identity is determined by a complex consisting of SEP and C-function proteins, while stamen identity is conferred by a complex composed of a B-class heterodimer, a C-function protein, and a SEP protein. Therefore, it is conceivable that a specific initial ratio between B- and C-gene expression levels is needed to result in final high levels of both B- and C-function proteins, which are required to favor the formation of a B/C/SEP stamen identity complex. According to this viewpoint, although B-repression is not fully released in a single *ben* mutant background, establishment of the B-function program in its sepals would be made possible, since no competition with the C-function genes occurs. By contrast, in a *bl ben* context, upregulation and maintenance of the B-function in the first whorl could be overruled by the C-function genes due to an unfavorable initial C/B ratio. In turn, the initial C/B ratio might be more balanced in a *ben rob bl* background to allow simultaneous B- and C-gene upregulation due to full release of B-function repression. Finally, Arabidopsis AP2 also negatively regulates *SEP3* expression in the first whorl, in addition to repressing *AP3* and *AGAMOUS* (Krogan et al., 2012). Further experiments will be required to determine to what extent *BEN* and the *ROB* genes also regulate the expression domain of the petunia *SEP* genes. If so, potential differences in SEP protein availability in the first whorl of *ben bl* versus *ben rob bl* mutants might further influence the final outcome of B- and C-gene upregulation.

Different Patterns of Functional Divergence in the *euAP2* Clade

All of the petunia *AP2*/*ERF* family members analyzed here (*BEN*, *BOB*, *ROB1*, *ROB2*, and *ROB3*) belong to the *euAP2* lineage, a subgroup within the large AP2/ERF family characterized by the presence of two AP2 domains and miR172 target sites (Kim et al., 2006). We showed that the petunia AP2-type genes *ROB1*, *ROB2*, and *ROB3* only pattern the B-function in the sepals, while Arabidopsis *AP2* was shown to regulate both the B- and C- function expression domains (Krogan et al., 2012). In turn, we found that petunia *BEN*, a TOE-type gene, regulates the B- and C-function expression domains as found for *AP2*. In addition, we showed that *BEN* and *BOB*, two closely related genes, are redundantly required for proper development of second and third floral whorls. In contrast, loss-of-function mutants for the Arabidopsis TOE-type genes (*TOE1*, *TOE2*, *SMZ*, and *SNZ*) do not display defects in floral organ development. Instead, all of these genes have been identified as floral repressors, together with *TOE3* and *AP2* (Aukerman and Sakai, 2003; Jung et al., 2007; Mathieu et al., 2009; Yant et al., 2010; Huijser and Schmid, 2011; Zhu and Helliwell, 2011). In turn, we did not observe obvious effects on flowering time in any of the single and higher order mutants we analyzed in this study, although we cannot exclude the possibility that we missed subtle phenotypes that might be difficult to observe in a greenhouse. On the other hand, petunia contains three other TOE-type genes (Figure 2M) that we have not yet functionally analyzed. Therefore, it is possible that at least some of the *euAP2* genes from petunia might function as floral repressors, possibly in a redundant fashion similar to that in Arabidopsis. Functional analysis of these uncharacterized genes and possibly the creation of higher order mutants will be needed to address this issue.

Although much more functional data from a wider range of species will be required to understand in detail the evolutionary trajectory of individual *euAP2* genes, the above data strongly suggest that different patterns of functional divergence in the *euAP2* clade have occurred in the lineages leading to Arabidopsis and petunia.

Thus, together with the identification of the *BL*/*FIS* functions in petunia and snapdragon, different patterns of functional divergence in the *euAP2* clade may help to explain why two decades of comparative flower development have failed to demonstrate molecular conservation of the Arabidopsis A-function in other species. One of the questions that now arises is whether this reflects a general difference between rosids and asterids. Although comparative studies are largely lacking, the available data thus far seem to support this. The distantly related asterid species snapdragon and petunia both employ the same *miRNA* (*FIS*/*BL*) as the major C-patterning factor, while their genes most similar to Arabidopsis *AP2* are required for normal floral organ development but are not involved in C-patterning. However, a B-patterning function for the snapdragon *LIP* genes remains to be shown, possibly still hidden in redundancy with *BEN* and/or other *AP2* homolog(s). Our findings now also offer a logical explanation for the striking phenotypic difference induced by *Pro35S:miR172* in Arabidopsis (Chen, 2004) compared with wild tobacco (*Nicotiana benthamiana*) (Mlotshwa et al., 2006), a close relative of petunia. While *Pro35S:miR172* flowers in Arabidopsis closely resemble strong *ap2* alleles, *N. benthamiana Pro35S:miR172* overexpression lines exhibited phenotypes ranging from the wild type to flowers resembling *ben* single mutants to *ben rob* higher order mutants. While the molecular basis of the phenotype was not analyzed, it is likely that *miR172* overexpression resulted in the codownregulation of *BEN* and *ROB* homologs in *N. benthamiana*, since they all share a *miR172* recognition site in their coding sequence (Supplemental Figure 2B). This suggests that a similar *BEN*/*ROB* dependent B-class patterning mechanism may also be active in other asterid species, at least in *N. benthamiana*.

Finally, it should be noted that in the original ABC model, the B-function expression domain was proposed to be independent from the A- and C-functions. The combinatorial nature and

complexity of the identified cadastral (boundary setting) functions in petunia (Figure 6A) are therefore difficult to integrate in the textbook ABC model. However, our findings are perfectly compatible with a more recent view of floral development, the (A)BC model (Causier et al., 2010), in which a more broadly defined (A)-function provides the genetic context in which the B- and C-functions are active and regulates both their spatial and temporal expression domains.

METHODS

Plant Material and Genotyping

Petunia (*Petunia hybrida* W138) plants were grown under standard greenhouse conditions (16 h day/8 h night; natural light supplemented with Philips Sodium HPS 400W SON-T AGRO light bulbs; 55,000 lumens) that were further influenced by local seasonal changes (45.72°N 4.82°E). The *bl-1* and *bl-2* alleles have been described earlier (Cartolano et al., 2007). The *ben* mutation was identified as spontaneous recessive mutation segregating in a *bl-1* family introgressed in the W138 background, a highly active *dTph1* transposon line that is commonly used for petunia mutagenesis (Vandenbussche et al., 2016). The *ben-139*, *ben-724*, *bob-213*, *bob-519*, *rob1-61*, *rob1-114*, *rob1-463F*, *rob1-463R*, *rob2-915*, and *rob3-935 dTph1* insertion alleles were all identified by BLAST searching our *dTph1* transposon flanking sequence database (Vandenbussche et al., 2008), which has been considerably enlarged in recent years. Note that the *dTph1* transposon is small (284 bp) and therefore does not necessarily affect gene function when inserted in promoter, untranslated region, or intron regions. For that reason, we exclusively selected and analyzed putative *dTph1* insertions in the coding sequences of *BEN*, *BOB*, *ROB1*, *ROB2*, and *ROB3.* When inserted in the coding sequence, the *dTph1* element is cotranscribed and normally leads to disruption of gene function, since *dTph1* contains multiple stop codons in all six possible reading frames. Insert positions (expressed in base pairs downstream of the ATG start codon with the coding sequence as a reference) were determined by aligning the *dTph1* flanking sequences with the genomic and cDNA sequences. All in silico-identified candidate insertions were confirmed by PCR-based genotyping of the progeny from the selected insertion lines, using primers flanking the *dTph1* transposon insertions. All segregation primers are listed in Supplemental Table 1. The following thermal profile was used for segregation analysis PCR: 11 cycles (94°C for 15 s, 71°C for 20 s minus 1°C/cycle, 72°C for 30 s), followed by 40 cycles (94°C for 15 s, 60°C for 20 s, and 72°C for 30 s). The different insertion mutants were further systematically genotyped in subsequent crosses and segregation analyses. Homozygous mutants were manually cross-pollinated for double, triple, and higher order mutant analyses. See Supplemental Table 4 for details on the phenotypic analysis. Insertion alleles used in the crosses are indicated in the corresponding figure legends.

Cloning of the *ben* Mutation by Transposon Display

To generate the required material for a transposon display experiment, all individuals of the *ben* segregating family that displayed a single mutant *bl-1* phenotype were self-pollinated, and progeny (20 individuals) were grown from each of these plants. From this plant material, we selected 12 homozygous *ben* mutants and 12 plants homozygous wild type for the *ben* mutation. DNA was harvested from these 24 plants and subjected to transposon display analysis (Van den Broeck et al., 1998; Vandenbussche et al., 2013). Transposon flanking sequence fragments that cosegregate with the *ben* genotype (absent in all homozygous wild-type plants, but present in all of the homozygous mutants) are good candidates to represent the mutated *ben* locus. Note that the W138 transposon line is highly active, and transposon excision from a given locus may occur at any moment. In the case of the *dTph1* transposon, the major source of mutations in W138, excision usually results in the formation of a disrupting footprint that maintains the mutation. Therefore, transposon flanking sequences that are absent in all homozygous wild-type plants but present in most (but not all) of the homozygous mutants are also plausible candidates to represent the mutated locus. Based on these selection criteria, we retained several candidates potentially corresponding to the *ben* locus. Because the transposon display analysis does not allow one to clearly discriminate between heterozygous and homozygous presence of the transposon, we performed a segregation analysis using gene-specific flanking primers to more rigorously test linkage of these transposon insertions to the *bl ben* phenotype. With one exception (see below), this led to the exclusion of all candidates, since in each case, *bl ben* mutants were found that were not homozygous mutant for the candidate insertion. This demonstrates that these insertions were closely linked to the *BEN* locus but were not the causative agent of the phenotype. A PCR segregation analysis of the remaining candidate, using *ben-488* genotyping primers flanking the insertion site (Supplemental Table 1) showed that all *bl ben* plants were homozygous mutant for the transposon insertion, except for plant #2, while none of the *bl* plants showed the insertion. Sequencing of the corresponding transposon flanking fragment showed that it corresponded to an insertion in the functionally uncharacterized *PhAP2B* gene. Sequencing of the PCR amplification products from *bl ben* mutants confirmed the position of the insertion in *PhAP2B* at base pair position 488 downstream of the ATG, and it also revealed that the absence of the transposon in *bl ben* plant #2 was caused by complete excision of the *dTph1* element, which left behind an 8-bp footprint, causing premature stop codons, and thus maintaining the mutation. Finally, segregation analysis of a larger selection of plants further confirmed a full linkage of the *phap2b* insertion with the *ben* phenotype in the *bl* background, as well as in outcrossed *ben* single mutants.

Imaging and Microscopy

Scanning electron microscopy images were obtained as previously described (Vandenbussche et al., 2009) or using a HIROX SH-1500 bench top environmental scanning electron microscope equipped with a cooled stage. Floral phenotypes were imaged by conventional digital photography using a glass plate as a support to generate a black background. When necessary, backgrounds were further equalized by removing dust particles and light reflections with Photoshop.

Identification of Petunia *euAP2* Genes and Phylogenetic Analysis

Petunia *euAP2* and *ANT* genes were identified among the predicted protein data sets from *Petunia axillaris* and *Petunia inflata* (Bombarely et al., 2016) by BLASTp using *euAP2* family members from *Arabidopsis thaliana* and tomato (*Solanum lycopersicum*), and in parallel by tBLASTN search against the *P. axillaris* and *P. inflata* genome sequences. Coding sequences of *BOB*, *ROB2*/*ROB3*, *ANT1*, and *ANT2* were experimentally determined by sequencing transcripts amplified from cDNA derived from young floral buds (W138 line) and deposited in GenBank (see Supplemental Table 3 for accession numbers). To evaluate the accuracy of the automatically predicted gene models of the petunia *euAP2* genes, we compared the translation of the experimentally obtained coding sequences of *BEN*, *BOB*, and *ROB1-3* with the gene models (Supplemental Figure 2A). For two out of the five genes (*ROB1* and *ROB3*), predictions were accurate, while for the remaining ones, some exons were absent or their borders not entirely correctly predicted (Supplemental Figure 2A). For the three TOE-type proteins that we did not functionally analyze in this study (Supplemental Table 3), but which were included in the phylogenetic analysis, we improved predictions for two of the *P. axillaris* copies based on alignments of the

genome sequence with RNA-seq data (Supplemental Table 3). The automatically predicted versions as well as our RNA-seq-based improved versions (marked with an asterisk at the end of the sequence name) are shown in the alignment of Supplemental Figure 2A. We retained the five experimentally defined W138 *euAP2* sequences and three remaining *P. axillaris* representatives (two of which were corrected) to be included in the phylogenetic analysis. Whole-genome predicted protein and transcript data sets of Arabidopsis, *Capsella rubella*, tomato, *Medicago truncatula*, grape (*Vitis vinifera*), and peach (*Prunus persica*) were downloaded from the Phytozome website (https://phytozome.jgi.doe.gov/pz/portal.html). These data sets were subjected to local BLAST analysis using BioEdit (Hall, 1999) for the identification and retrieval of euAP2 protein and nucleotide sequences. The tomato SlAP2 sequences (Supplemental Table 3) were retrieved from GenBank. Alignments were obtained using ClustalW (Thompson et al., 1994) and were further manually refined in BioEdit (see Supplemental File 1). Start and end of the partial sequences of the Arabidopsis and petunia AINTEGUMENTA (ANT) proteins shown in Supplemental Figure 2B mark the conserved region that was used to generate the neighbor-joining tree shown in Figure 2M. The tree was computed with Treecon software (Van de Peer and De Wachter, 1994) using the following settings: (1) distance estimation options: Tajima and Nei distance calculation; insertions and deletion not taken into account; alignment positions: all; bootstrap analysis: yes, 2000 samples. (2) Infer tree topology options: neighbor-joining; bootstrap analysis: yes. (3) Root unrooted trees options: outgroup option: single sequence (forced); bootstrap analysis: yes; select root: At-ANT. The two major lineages of AP2-like genes consist of euAP2 and ANT genes (Kim et al., 2006). We therefore opted to root the euAP2 tree with ANT proteins. Positions of the two conserved AP2 domains (Figures 2C, 3B, and 4B) were determined via the NCBI CCD database (http://www.ncbi.nlm.nih.gov/Structure/cdd/wrpsb.cgi).

Expression Analysis

For qRT-PCR analysis, tissues were ground in liquid nitrogen, and total RNA was extracted using Trizol reagent (Invitrogen) and treated with Turbo DNA-free DNase I (Ambion). RNA was reverse transcribed using RevertAid M-MuLV reverse transcriptase (Fermentas) according to the manufacturer's protocol. PCR was performed in an optical 384-well plate in the QuantStudio 6 Flex real-time PCR system (Applied Biosystems) using FastStart Universal SYBR Green Master (Rox) (Roche), in a final volume of 10 μL, according to the manufacturer's instructions. Primers used were designed using the online Universal ProbeLibrary Assay Design Center (Roche). All primers are listed in Supplemental Table 1. The following standard thermal profile was used for all PCR: 95°C for 10 min, 40 cycles of 95°C for 10 s, and 60°C for 30 s. Data were analyzed using QuantStudio 6 and 7 Flex Real-Time PCR System Software v1.0 (Applied Biosystems). PCR efficiency (*E*) was estimated from the data obtained from standard curve amplification using the equation $E = 10^{-1}/slope$. Relative expression (R.E.) values on the *y* axes are the average of nine data points resulting from the technical triplicates of three biological replicates ± SD and normalized to the geometrical average of three $E^{-\Delta Ct}$, where $\Delta Ct = Ct_{GOI} - Ct_{ACTIN,\ GAPDH\ or\ RAN}$. The floral bud series (marked floral buds 1–3 in Figures 2D, 3A, and 4A) are successive developmental stages of complete floral buds harvested from the same inflorescences (Supplemental Figure 1). For each biological replicate, corresponding stages harvested from three inflorescences were pooled. Stage 3 corresponds to flower buds with a diameter of ~5 mm and from which individual floral organs can be easily dissected by hand. All analyses showing expression in separate floral organ types are from this stage. Biological replicates of the different floral organ types were composed of pooled stage 3 organs harvested from three different flowers each time. For mutants with highly modified floral architecture, developmental stages in relation to wild-type development were deduced based on their position on the inflorescence. Floral buds marked "2" (diameter ~2.5 mm) and "1" (diameter ~1.5 mm) are younger stages and were harvested from the next two nodes produced after bud stage 3. In addition to 1.5-mm buds, stage 1 also includes the inflorescence meristem and very young developing floral primordia subtended by bracts, which are attached to the base of the pedicel of the 1.5-mm bud. Vegetative apices (including very small leaf primordia) were harvested from 3-week-old seedlings by manually removing cotyledons, roots, and developed leaves. Young leaf primordia were isolated from the same 3-week-old seedlings. Each biological replicate of the vegetative apices and young leaf primordia consisted of pooled material harvested from each time 10 seedlings. In situ hybridization of *PhGLO2* (Figure 5L) was done as described previously (Vandenbussche et al., 2004).

Accession Numbers

Sequence data from this article can be found in the GenBank/EMBL libraries under accession numbers KU096994, KU096995, KU096996, KU096997, KU096998, KU096994, MF327594, and MF327595 (see also Supplemental Table 3).

Supplemental Data

Supplemental Figure 1. W138 Floral Bud Developmental Stages Sampled for qRT-PCR Analysis.

Supplemental Figure 2. Alignments of *euAP2* Protein Sequences from Petunia and Other Selected Species.

Supplemental Figure 3. Additional *rob* and *ben rob* Mutant Phenotypes.

Supplemental Table 1. Oligo Sequences Used in This Study

Supplemental Table 2. Sequence comparison of Petunia BEN, BOB, and ROB1-3 against the Six Arabidopsis *euAP2* Protein Sequences (TAIR10 Database).

Supplemental Table 3. Gene Names, Synonyms, and Accession Codes for Sequences Shown in Figure 2M and Supplemental Figure 2.

Supplemental Table 4. Overview of Genotypes Analyzed in This Study.

Supplemental File 1. Alignment of euAP2 Protein Sequences from Petunia (Ph; Peaxi), Tomato (Sl; Sol), Arabidopsis (At), *Capsella rubella* (Carub), *Medicago truncatula* (Medtr), Grape (GSVIV), and peach (Prupe) in Fasta Format.

ACKNOWLEDGMENTS

M.V. was supported by a CNRS ATIP-AVENIR award. K.H. was supported by NWO Grant 818.02.012. We thank A. Lacroix and J. Berger for plant care assistance and V. Bayle for electron microscopy technical support.

AUTHOR CONTRIBUTIONS

M.V., P.M., and K.H. conceived and designed the experiments. P.M., K.H., J.Z., F.R., S.C., S.R.B., A.V.-G., P.C., C.T., and M.V. performed the experiments. P.M., K.H., and M.V. analyzed the data. M.V., K.H., and P.M. wrote the article with feedback from C.T. and A.V.-G.

Received February 6, 2017; revised May 8, 2017; accepted June 20, 2017; published June 23, 2017.

REFERENCES

Angenent, G.C., Franken, J., Busscher, M., Colombo, L., and van Tunen, A.J. (1993). Petal and stamen formation in petunia is regulated by the homeotic gene fbp1. Plant J. **4:** 101–112.

Aukerman, M.J., and Sakai, H. (2003). Regulation of flowering time and floral organ identity by a MicroRNA and its APETALA2-like target genes. Plant Cell **15:** 2730–2741.

Bombarely, A., et al. (2016). Insight into the evolution of the Solanaceae from the parental genomes of *Petunia hybrida*. Nat. Plants **2:** 16074.

Bowman, J.L., Smyth, D.R., and Meyerowitz, E.M. (1991). Genetic interactions among floral homeotic genes of Arabidopsis. Development **112:** 1–20.

Bradley, D., Carpenter, R., Sommer, H., Hartley, N., and Coen, E. (1993). Complementary floral homeotic phenotypes result from opposite orientations of a transposon at the plena locus of Antirrhinum. Cell **72:** 85–95.

Cartolano, M., Castillo, R., Efremova, N., Kuckenberg, M., Zethof, J., Gerats, T., Schwarz-Sommer, Z., and Vandenbussche, M. (2007). A conserved microRNA module exerts homeotic control over *Petunia hybrida* and *Antirrhinum majus* floral organ identity. Nat. Genet. **39:** 901–905.

Causier, B., Schwarz-Sommer, Z., and Davies, B. (2010). Floral organ identity: 20 years of ABCs. Semin. Cell Dev. Biol. **21:** 73–79.

Causier, B., Castillo, R., Zhou, J., Ingram, R., Xue, Y., Schwarz-Sommer, Z., and Davies, B. (2005). Evolution in action: following function in duplicated floral homeotic genes. Curr. Biol. **15:** 1508–1512.

Chen, X. (2004). A microRNA as a translational repressor of APETALA2 in Arabidopsis flower development. Science **303:** 2022–2025.

Coen, E.S., and Meyerowitz, E.M. (1991). The war of the whorls: genetic interactions controlling flower development. Nature **353:** 31–37.

Dinh, T.T., Girke, T., Liu, X., Yant, L., Schmid, M., and Chen, X. (2012). The floral homeotic protein APETALA2 recognizes and acts through an AT-rich sequence element. Development **139:** 1978–1986.

Drews, G.N., Bowman, J.L., and Meyerowitz, E.M. (1991). Negative regulation of the Arabidopsis homeotic gene AGAMOUS by the APETALA2 product. Cell **65:** 991–1002.

Gerats, A.G., Huits, H., Vrijlandt, E., Maraña, C., Souer, E., and Beld, M. (1990). Molecular characterization of a nonautonomous transposable element (dTph1) of petunia. Plant Cell **2:** 1121–1128.

Gómez-Mena, C., de Folter, S., Costa, M.M., Angenent, G.C., and Sablowski, R. (2005). Transcriptional program controlled by the floral homeotic gene AGAMOUS during early organogenesis. Development **132:** 429–438.

Goto, K., and Meyerowitz, E.M. (1994). Function and regulation of the *Arabidopsis* floral homeotic gene *PISTILLATA.* Genes Dev. **8:** 1548–1560.

Hall, T.A. (1999). BioEdit: A user-friendly biological sequence alignment editor and analysis program for Windows 95/98/NT. Nucleic Acids Symp. Ser. **41:** 95–98.

Heijmans, K., Ament, K., Rijpkema, A.S., Zethof, J., Wolters-Arts, M., Gerats, T., and Vandenbussche, M. (2012). Redefining C and D in the petunia ABC. Plant Cell **24:** 2305–2317.

Hong, R.L., Hamaguchi, L., Busch, M.A., and Weigel, D. (2003). Regulatory elements of the floral homeotic gene AGAMOUS identified by phylogenetic footprinting and shadowing. Plant Cell **15:** 1296–1309.

Huijser, P., and Schmid, M. (2011). The control of developmental phase transitions in plants. Development **138:** 4117–4129.

Jack, T., Brockman, L.L., and Meyerowitz, E.M. (1992). The homeotic gene *APETALA3* of Arabidopsis thaliana encodes a MADS box and is expressed in petals and stamens. Cell **68:** 683–697.

Jaillon, O., et al.; French-Italian Public Consortium for Grapevine Genome Characterization (2007) The grapevine genome sequence suggests ancestral hexaploidization in major angiosperm phyla. Nature **449:** 463–467.

Jofuku, K.D., den Boer, B.G., Van Montagu, M., and Okamuro, J.K. (1994). Control of Arabidopsis flower and seed development by the homeotic gene APETALA2. Plant Cell **6:** 1211–1225.

Jones-Rhoades, M.W., and Bartel, D.P. (2004). Computational identification of plant microRNAs and their targets, including a stress-induced miRNA. Mol. Cell **14:** 787–799.

Jung, J.H., Seo, Y.H., Seo, P.J., Reyes, J.L., Yun, J., Chua, N.H., and Park, C.M. (2007). The GIGANTEA-regulated microRNA172 mediates photoperiodic flowering independent of CONSTANS in Arabidopsis. Plant Cell **19:** 2736–2748.

Kapoor, M., Tsuda, S., Tanaka, Y., Mayama, T., Okuyama, Y., Tsuchimoto, S., and Takatsuji, H. (2002). Role of petunia *pMADS3* in determination of floral organ and meristem identity, as revealed by its loss of function. Plant J. **32:** 115–127.

Kater, M.M., Colombo, L., Franken, J., Busscher, M., Masiero, S., Van Lookeren Campagne, M.M., and Angenent, G.C. (1998). Multiple *AGAMOUS* homologs from cucumber and petunia differ in their ability to induce reproductive organ fate. Plant Cell **10:** 171–182.

Kaufmann, K., Muiño, J.M., Jauregui, R., Airoldi, C.A., Smaczniak, C., Krajewski, P., and Angenent, G.C. (2009). Target genes of the MADS transcription factor SEPALLATA3: integration of developmental and hormonal pathways in the Arabidopsis flower. PLoS Biol. **7:** e1000090.

Keck, E., McSteen, P., Carpenter, R., and Coen, E. (2003). Separation of genetic functions controlling organ identity in flowers. EMBO J. **22:** 1058–1066.

Kim, S., Soltis, P.S., Wall, K., and Soltis, D.E. (2006). Phylogeny and domain evolution in the APETALA2-like gene family. Mol. Biol. Evol. **23:** 107–120.

Krizek, B.A., and Fletcher, J.C. (2005). Molecular mechanisms of flower development: an armchair guide. Nat. Rev. Genet. **6:** 688–698.

Krogan, N.T., Hogan, K., and Long, J.A. (2012). APETALA2 negatively regulates multiple floral organ identity genes in Arabidopsis by recruiting the co-repressor TOPLESS and the histone deacetylase HDA19. Development **139:** 4180–4190.

Kunst, L., Klenz, J.E., Martinez-Zapater, J., and Haughn, G.W. (1989). AP2 gene determines the identity of perianth organs in flowers of *Arabidopsis thaliana*. Plant Cell **1:** 1195–1208.

Litt, A. (2007). An evaluation of A-function: Evidence from the *APETALA1* and *APETALA2* gene lineages. Int. J. Plant Sci. **168:** 73–91.

Maes, T., Van de Steene, N., Zethof, J., Karimi, M., D'Hauw, M., Mares, G., Van Montagu, M., and Gerats, T. (2001). Petunia Ap2-like genes and their role in flower and seed development. Plant Cell **13:** 229–244.

Mantovani, R. (1999). The molecular biology of the CCAAT-binding factor NF-Y. Gene **239:** 15–27.

Mathieu, J., Yant, L.J., Mürdter, F., Küttner, F., and Schmid, M. (2009). Repression of flowering by the miR172 target SMZ. PLoS Biol. **7:** e1000148.

McSteen, P.C., Vincent, C.A., Doyle, S., Carpenter, R., and Coen, E.S. (1998). Control of floral homeotic gene expression and organ morphogenesis in *Antirrhinum.* Development **125:** 2359–2369.

Mlotshwa, S., Yang, Z., Kim, Y., and Chen, X. (2006). Floral patterning defects induced by Arabidopsis APETALA2 and microRNA172 expression in *Nicotiana benthamiana*. Plant Mol. Biol. **61:** 781–793.

Moore, M.J., Soltis, P.S., Bell, C.D., Burleigh, J.G., and Soltis, D.E. (2010). Phylogenetic analysis of 83 plastid genes further resolves the early diversification of eudicots. Proc. Natl. Acad. Sci. USA **107:** 4623–4628.

Rijpkema, A.S., Royaert, S., Zethof, J., van der Weerden, G., Gerats, T., and Vandenbussche, M. (2006). Analysis of the *Petunia TM6* MADS box gene reveals functional divergence within the *DEF/AP3* lineage. Plant Cell **18:** 1819–1832.

Slotte, T., et al. (2013). The Capsella rubella genome and the genomic consequences of rapid mating system evolution. Nat. Genet. **45:** 831–835.

Sommer, H., Beltrán, J.P., Huijser, P., Pape, H., Lönnig, W.E., Saedler, H., and Schwarz-Sommer, Z. (1990). Deficiens, a homeotic gene involved in the control of flower morphogenesis in *Antirrhinum majus*: the protein shows homology to transcription factors. EMBO J. **9:** 605–613.

Theissen, G., and Saedler, H. (2001). Plant biology. Floral quartets. Nature **409:** 469–471.

Thompson, J.D., Higgins, D.G., and Gibson, T.J. (1994). CLUSTAL W: improving the sensitivity of progressive multiple sequence alignment through sequence weighting, position-specific gap penalties and weight matrix choice. Nucleic Acids Res. **22:** 4673–4680.

Tomato Genome Consortium (2012). The tomato genome sequence provides insights into fleshy fruit evolution. Nature **485:** 635–641.

Tröbner, W., Ramirez, L., Motte, P., Hue, I., Huijser, P., Lönnig, W.E., Saedler, H., Sommer, H., and Schwarz-Sommer, Z. (1992). GLOBOSA: a homeotic gene which interacts with DEFICIENS in the control of Antirrhinum floral organogenesis. EMBO J. **11:** 4693–4704.

Tsuchimoto, S., van der Krol, A.R., and Chua, N.H. (1993). Ectopic expression of *pMADS3* in transgenic petunia phenocopies the petunia *blind* mutant. Plant Cell **5:** 843–853.

Vallade, J., Maizonnier, D., and Cornu, A. (1987). La morphogenèse florale chez le pétunia. I. Analyse d'un mutant à corolle staminée. Can. J. Bot. **65:** 761–764.

Van den Broeck, D., Maes, T., Sauer, M., Zethof, J., De Keukeleire, P., D'hauw, M., Van Montagu, M., and Gerats, T. (1998). Transposon display identifies individual transposable elements in high copy number lines. Plant J. **13:** 121–129.

Vandenbussche, M., Zethof, J., and Gerats, T. (2013). Transposon display: a versatile method for transposon tagging. Methods Mol. Biol. **1057:** 239–250.

Vandenbussche, M., Chambrier, P., Rodrigues Bento, S., and Morel, P. (2016). Petunia, your next supermodel? Front. Plant Sci. **7:** 72.

Vandenbussche, M., Zethof, J., Royaert, S., Weterings, K., and Gerats, T. (2004). The duplicated B-class heterodimer model: whorl-specific effects and complex genetic interactions in *Petunia hybrida* flower development. Plant Cell **16:** 741–754.

Vandenbussche, M., Horstman, A., Zethof, J., Koes, R., Rijpkema, A.S., and Gerats, T. (2009). Differential recruitment of WOX transcription factors for lateral development and organ fusion in Petunia and Arabidopsis. Plant Cell **21:** 2269–2283.

Vandenbussche, M., Janssen, A., Zethof, J., van Orsouw, N., Peters, J., van Eijk, M.J., Rijpkema, A.S., Schneiders, H., Santhanam, P., de Been, M., van Tunen, A., and Gerats, T. (2008). Generation of a 3D indexed petunia insertion database for reverse genetics. Plant J. **54:** 1105–1114.

Van de Peer, Y., and De Wachter, R. (1994). TREECON for Windows: a software package for the construction and drawing of evolutionary trees for the Microsoft Windows environment. Comput. Appl. Biosci. **10:** 569–570.

van der Krol, A.R., Brunelle, A., Tsuchimoto, S., and Chua, N.H. (1993). Functional analysis of petunia floral homeotic MADS box gene pMADS1. Genes Dev. **7:** 1214–1228.

Verde, I., et al.; International Peach Genome Initiative (2013) The high-quality draft genome of peach (Prunus persica) identifies unique patterns of genetic diversity, domestication and genome evolution. Nat. Genet. **45:** 487–494.

Wang, P., Cheng, T., Lu, M., Liu, G., Li, M., Shi, J., Lu, Y., Laux, T., and Chen, J. (2016). Expansion and functional divergence of AP2 group genes in spermatophytes determined by molecular evolution and Arabidopsis mutant analysis. Front. Plant Sci. **7:** 1383.

Wollmann, H., Mica, E., Todesco, M., Long, J.A., and Weigel, D. (2010). On reconciling the interactions between APETALA2, miR172 and AGAMOUS with the ABC model of flower development. Development **137:** 3633–3642.

Yanofsky, M.F., Ma, H., Bowman, J.L., Drews, G.N., Feldmann, K.A., and Meyerowitz, E.M. (1990). The protein encoded by the Arabidopsis homeotic gene agamous resembles transcription factors. Nature **346:** 35–39.

Yant, L., Mathieu, J., Dinh, T.T., Ott, F., Lanz, C., Wollmann, H., Chen, X., and Schmid, M. (2010). Orchestration of the floral transition and floral development in Arabidopsis by the bifunctional transcription factor APETALA2. Plant Cell **22:** 2156–2170.

Young, N.D., et al. (2011). The Medicago genome provides insight into the evolution of rhizobial symbioses. Nature **480:** 520–524.

Zhu, Q.H., and Helliwell, C.A. (2011). Regulation of flowering time and floral patterning by miR172. J. Exp. Bot. **62:** 487–495.